



**HAL**  
open science

# Hepatitis C Virus-Induced Upregulation of MicroRNA miR-146a-5p in Hepatocytes Promotes Viral Infection and Deregulates Metabolic Pathways Associated with Liver Disease Pathogenesis

Simonetta Bandiera, Sophie Pernot, Hussein El Saghire, Sarah Durand, Christine Thumann, Emilie Crouchet, Tao Ye, Isabel Fofana, Marine Oudot, Jochen Barths, et al.

► **To cite this version:**

Simonetta Bandiera, Sophie Pernot, Hussein El Saghire, Sarah Durand, Christine Thumann, et al.. Hepatitis C Virus-Induced Upregulation of MicroRNA miR-146a-5p in Hepatocytes Promotes Viral Infection and Deregulates Metabolic Pathways Associated with Liver Disease Pathogenesis. *Journal of Virology*, 2016, 90 (14), pp.6387-6400. 10.1128/JVI.00619-16 . hal-02372996

**HAL Id: hal-02372996**

**<https://hal.science/hal-02372996>**

Submitted on 27 Mar 2023

**HAL** is a multi-disciplinary open access archive for the deposit and dissemination of scientific research documents, whether they are published or not. The documents may come from teaching and research institutions in France or abroad, or from public or private research centers.

L'archive ouverte pluridisciplinaire **HAL**, est destinée au dépôt et à la diffusion de documents scientifiques de niveau recherche, publiés ou non, émanant des établissements d'enseignement et de recherche français ou étrangers, des laboratoires publics ou privés.

1           **HCV-induced up-regulation of miR-146a-5p in hepatocytes**  
2           **promotes viral infection and deregulates metabolic pathways**  
3           **associated with liver disease pathogenesis**

4  
5  
6           Simonetta Bandiera<sup>1,2,\*</sup>, Sophie Pernot<sup>1,2,\*</sup>, Hussein El Saghire<sup>1,2</sup>,  
7           Sarah C. Durand<sup>1,2</sup>, Christine Thumann<sup>1,2</sup>, Emilie Crouchet<sup>1,2</sup>, Tao Ye<sup>2,3</sup>,  
8           Isabel Fofana<sup>4</sup>, Marine A. Oudot<sup>1,2</sup>, Jochen Barths<sup>1,2</sup>, Catherine Schuster<sup>1,2</sup>,  
9           Patrick Pessaux<sup>1,2,5</sup>, Markus H. Heim<sup>4</sup>, Thomas F. Baumert<sup>1,2,5,#</sup>, Mirjam B. Zeisel<sup>1,2,#</sup>

10  
11           <sup>1</sup>Inserm, U1110, Institut de Recherche sur les Maladies Virales et Hépatiques,  
12           Strasbourg, France; <sup>2</sup>Université de Strasbourg, Strasbourg, France; <sup>3</sup>Institut de  
13           Génétique et de Biologie Moléculaire et Cellulaire, Illkirch, France; CNRS, UMR7104,  
14           Illkirch, France; Inserm, U964, Illkirch, France; <sup>4</sup>Division of Gastroenterology and  
15           Hepatology, University Hospital Basel, Basel, Switzerland; Department of  
16           Biomedicine, University of Basel, Basel, Switzerland; <sup>5</sup>Institut Hospitalo-Universitaire,  
17           Pôle Hépato-digestif, Hôpitaux Universitaires de Strasbourg, Strasbourg, France

18           \* these authors contributed equally

19  
20           **Word count.** Abstract: 250 words; Importance: 150 words; main manuscript: 5344  
21           words; 74 references; 5 figures; 2 tables

22  
23           **# Corresponding authors:** Mirjam B. Zeisel, PhD, PharmD, Inserm U1110,  
24           Université de Strasbourg, 3 Rue Koeberlé, F-67000 Strasbourg, France; Phone:  
25           (++33) 3 68 85 37 03, Fax: (++33) 3 68 85 37 24, e-mail: [Mirjam.Zeisel@unistra.fr](mailto:Mirjam.Zeisel@unistra.fr)

26 and Thomas F. Baumert, MD, Inserm U1110, Université de Strasbourg, 3 Rue  
27 Koeberlé and Pôle Hépatodigestif, Nouvel Hôpital Civil, F-67000 Strasbourg,  
28 France; Phone: (++33) 3 68 85 37 03, Fax: (++33) 3 68 85 37 24, e-mail:  
29 [Thomas.Baumert@unistra.fr](mailto:Thomas.Baumert@unistra.fr)

30

31 **Keywords.** Hepatitis C virus, microRNA, virus-host interactions, liver disease,  
32 hepatocellular carcinoma

33

34 **Running title.** Role of miR-146a-5p in HCV infection and pathogenesis (53  
35 characters)

36

37 **Abbreviations.** ACHP: 2-Amino-6-[2-(cyclopropylmethoxy)-6-hydroxyphenyl]-4-(4-  
38 piperidinyl)-3-pyridinecarbonitrile; AGCC: Affymetrix GeneChip® Command Console;  
39 ALS: amyotrophic lateral sclerosis; ANOVA: analysis of variance; apoE:  
40 apolipoprotein E; ASH: alcoholic steatohepatosis; CpG: cytidine-phosphate-  
41 guanosine; CXCL8: C-X-C motif chemokine ligand 8; DAA: direct-acting antiviral;  
42 DCV: daclatasvir; DMEM: Dulbecco's Modified Eagle Medium; DMSO: dimethyl  
43 sulfoxide; dpi: days post-infection; ECM: extracellular matrix; EGFR: epidermal  
44 growth factor receptor; KEGG: Kyoto Encyclopedia of Genes and Genomes; GSEA:  
45 Gene Set Enrichment Analysis; h: hours; HBV: hepatitis B virus; HCV: hepatitis C  
46 virus; HCVcc: cell culture-derived HCV; HCVpp: HCV pseudoparticles; HNF1a:  
47 hepatocyte nuclear factor 1a; HSC: human stellate cells; IKK: I $\kappa$ B kinase; IPA:  
48 Ingenuity Pathway Analysis; IRAK1: interleukin-1 receptor-associated kinase 1; JAK:  
49 Janus kinase; LPS: lipopolysaccharide; MAPK: mitogen-activated protein kinase;  
50 miRNA: microRNA; NASH: nonalcoholic steatohepatosis; NF- $\kappa$ B: nuclear factor

51 kappa B; NK: natural killer; NOD: nucleotide-binding oligomerization domain; nt:  
52 nucleotide; NS3: HCV nonstructural protein 3; NS5A: HCV nonstructural protein 5A;  
53 NS5B: HCV nonstructural protein 5B; PBMC: peripheral blood mononuclear cells;  
54 PBS: phosphate buffered saline; PHH: primary human hepatocyte; RIG: retinoic acid-  
55 inducible gene; RMA: Robust Multi-Array Average; RNA-Seq: RNA-sequencing,  
56 SHP-1: SH2 domain-containing phosphatase-1; RT-qPCR: Reverse Transcription  
57 Real-Time quantitative PCR; siRNA: small interfering RNA; SMV: simeprevir;  
58 SNORD61: small nucleolar RNA, C/D box 61; SOF: sofosbuvir; STAT3: signal  
59 transducer and activator of transcription 3; TCID<sub>50</sub>: 50 % tissue culture infectious  
60 dose; TLR: Toll-like receptor; VSVpp: vesicular stomatitis virus pseudoparticles  
61

62 **Abstract**

63 Hepatitis C virus (HCV)-induced chronic liver disease is a leading cause of  
64 hepatocellular carcinoma (HCC). However, the molecular mechanisms underlying  
65 HCC development following chronic HCV infection remain poorly understood.  
66 MicroRNAs (miRNAs) play an important role in homeostasis within the liver and  
67 deregulation of the miRNome has been associated with liver disease including HCC.  
68 While host miRNAs are essential for HCV replication, viral infection in turn appears to  
69 induce alterations of intrahepatic miRNA networks. Although the cross-talk between  
70 HCV and liver cell miRNAs most likely contributes to liver disease pathogenesis, the  
71 functional involvement of miRNAs in HCV-driven hepatocyte injury and HCC remains  
72 elusive. Here, we combined a hepatocyte-like based model system, high-throughput  
73 small RNA-sequencing, computational analysis and functional studies to investigate  
74 HCV-miRNA interactions that may contribute to liver disease and HCC. Profiling  
75 analyses indicated that HCV infection differentially regulated the expression of 72  
76 miRNAs by at least two-fold including miRNAs that were previously described to  
77 target genes associated with inflammation, fibrosis and cancer development. Further  
78 investigation demonstrated that miR-146a-5p was consistently increased in HCV-  
79 infected hepatocyte-like cells and primary human hepatocytes as well as in liver  
80 tissue from HCV-infected patients. Genome-wide microarray and computational  
81 analyses indicated that miR-146a-5p over-expression modulates pathways that are  
82 related to liver disease and HCC development. Furthermore, we showed that miR-  
83 146a-5p positively impacts on late steps of the viral replication cycle thereby  
84 increasing HCV infection. Collectively, our data indicate that the HCV-induced  
85 increase in miR-146a-5p expression both promotes viral infection and is relevant for  
86 pathogenesis of liver disease.

87 **Importance**

88 HCV is a leading cause of chronic liver disease and cancer. However, how HCV  
89 induces liver cancer remains poorly understood. There is accumulating evidence that  
90 viral cure does not eliminate the risk for HCC development. Thus, there is an unmet  
91 medical need to develop novel approaches to predict and prevent virus-induced  
92 HCC. miRNA expression is known to be deregulated in liver disease and cancer.  
93 Furthermore, miRNAs are essential for HCV replication and HCV infection alters  
94 miRNA expression. However, how miRNAs contribute to HCV-driven pathogenesis  
95 remains elusive. Here, we show that HCV induces miRNAs that may contribute to  
96 liver injury and carcinogenesis. miR-146a-5p was consistently increased in different  
97 cell-based models of HCV infection and HCV patient-derived liver tissue.  
98 Furthermore, miR-146a-5p increases HCV infection. Collectively, our data are  
99 relevant to understand viral pathogenesis and may open perspectives for novel  
100 biomarkers and prevention of virus-induced liver disease and HCC.

101 **Introduction**

102 HCV infection is a leading cause of chronic liver disease and HCC worldwide. While  
103 there is no vaccine to prevent HCV infection, tremendous progress has been made in  
104 the management of chronic hepatitis C (1). However, recent evidence indicates that  
105 individuals that have achieved viral cure remain at risk to develop HCC (2). This  
106 suggests that the virus triggers changes in host cell networks that drive liver disease  
107 and carcinogenesis, and persist even after viral elimination. However, the molecular  
108 mechanisms underlying HCV-induced liver disease and HCC development remain  
109 poorly understood.

110 miRNAs are small non-coding RNAs that regulate gene expression at a post-  
111 transcriptional level. They play an important role in cellular homeostasis within the  
112 liver and hence alterations in intrahepatic miRNA networks have been associated  
113 with liver disease, including fibrosis, cirrhosis and HCC (3, 4). Notably, HCV infection  
114 is intricately linked to miRNAs as the most abundant miRNA of the liver, miR-122, is  
115 essential for HCV replication (5-7). In addition of using host miRNAs for viral  
116 replication, HCV may also modulate host cell miRNA profiles to favour its  
117 persistence, and thereby induce liver disease (8). Accumulating evidence highlights a  
118 complex cross-talk between HCV and miRNAs in liver fibrosis, steatosis and HCC  
119 (8). However, the functional involvement of miRNAs in HCV-mediated hepatocyte  
120 injury and liver disease pathogenesis remains to be elucidated.

121 Several pieces of evidence have shown HCV-mediated deregulation of  
122 miRNAs in hepatoma cell lines (9). Although a few *ex vivo* studies have investigated  
123 miRNA patterns in HCV-associated HCC tissues, no clear picture has yet emerged  
124 as to the modulation of miRNAs upon HCV-induced liver disease. Indeed, these  
125 studies largely differ in their methodological approach, the sampling size and

126 features, and the ethnicity of patients (9, 10). Most importantly, only limited  
127 information is available about the differential expression of miRNAs in pre-neoplastic  
128 liver nodules as compared to HCC (11, 12), underlying the current lack of a proper  
129 model that closely recapitulates the progression of HCV-associated HCC. To date,  
130 the majority of cell culture models to study the molecular virology and cell biology of  
131 HCV infection rely on human hepatoma cells (reviewed in (13)). However, given their  
132 transformed phenotype, these model systems may preclude systematic identification  
133 of the changes in host cell circuits that are relevant for virus-induced liver disease.  
134 Human hepatocytes are the natural target cells of HCV, but primary cells are not well  
135 suited for large scale and long-term analysis of infection. It had previously been  
136 reported that dimethyl sulfoxide (DMSO)-differentiation of Huh7-derived human  
137 hepatoma cell lines induces a hepatocyte-like phenotype and that these cells are  
138 amenable to long-term HCV infection (14-16). In this study, we combined this  
139 hepatocyte-like based model system, high-throughput small RNA-sequencing (RNA-  
140 Seq), computational analysis and functional studies to investigate HCV-miRNA  
141 interactions that may contribute to liver disease and HCC.

142

## 143 **Material and method**

### 144 ***Reagents***

145 DMSO was from Sigma Aldrich. DAPI was obtained from Life Technologies. HCV E2-  
146 specific AP33 antibody (mouse) has been described (17). The ACHP inhibitor was  
147 obtained from Tocris. Direct-acting antivirals (DAAs) daclatasvir (DCV; NS5A  
148 inhibitor), sofosbuvir (SOF; NS5B inhibitor) and simeprevir (SMV; NS3 inhibitor) were  
149 synthesized by Acme Bioscience. miR-146a-5p mimic was from Sigma Aldrich. Anti-  
150 miR-146a-5p was synthesized by Integrated DNA Technology (IDT). Non-targeting

151 control siRNA, miR-122-5p mimic, anti-miR-122, siRNAs targeting *CD81* or  
152 *apolipoprotein E* (apoE) were from Dharmacon (GE Healthcare). siRNA targeting  
153 *signal transducer and activator of transcription 3 (STAT3)* was obtained from Qiagen.

154

#### 155 **Cell culture**

156 The source and culture conditions of Huh7.5.1, Huh7 and HEK293T cells have been  
157 described (18). For proliferation arrest and differentiation in long-term infection  
158 experiments,  $2.5 \times 10^4$  Huh7.5.1 cells were cultured in Dulbecco's Modified Eagle  
159 Medium (DMEM) containing 1% DMSO as described for Huh7 and Huh7.5 cells (14-  
160 16). Primary human hepatocytes (PHH) were isolated and cultured as described (19).

161

#### 162 **Human subjects**

163 Human material from patients undergoing liver biopsy or surgical resection was  
164 obtained with informed consent from all patients. The respective protocols were  
165 approved by the Ethics Committee of the University Hospital of Basel, Switzerland  
166 (EKBB 13 December 2004, liver biopsies) and University of Strasbourg Hospitals,  
167 France (CPP 10-17, primary human hepatocytes).

168

#### 169 **Liver biopsies**

170 Histopathological grading and staging of the liver biopsies according to the Metavir  
171 classification system was performed at the Pathology Institute of the University  
172 Hospital Basel as described (20) and are summarized in Table 1. All patients that  
173 donated liver tissue were male between 30 and 70 years old and female between 31  
174 and 76 years old (Table 1).

175

176 ***HCV production and infection assays***

177 HCV pseudoparticles (HCVpp) expressing envelope glycoproteins from strain J6  
178 (genotype 2a) and harboring a luciferase reporter gene were generated as described  
179 (21, 22). Huh7.5.1 cells were incubated with HCVpp and HCV entry was assessed by  
180 measuring luciferase activity 3 days later as described (19). Vesicular stomatitis virus  
181 pseudoparticles (VSVpp) were assessed in parallel as an unrelated virus (21, 22).  
182 Cell culture-derived (HCVcc) Jc1, Jc1E2<sup>FLAG</sup> and JcR2a (all derived from the J6/JFH1  
183 chimera Jc1, genotype 2a/2a) were generated in Huh7.5.1 cells as described (23-  
184 25). Infectivity of HCVcc was determined by calculating the 50% tissue culture  
185 infectious doses (TCID<sub>50</sub>) as described (26). Titers of HCVcc Jc1 and JcR2a used  
186 across experiments were ~10<sup>6</sup>/mL, and titer of Jc1E2<sup>FLAG</sup> for the RNA-seq experiment  
187 was 1.6 x 10<sup>7</sup>/mL. Fifty-percent confluent Huh7.5.1 cultures were infected with  
188 HCVcc Jc1 or Jc1E2<sup>FLAG</sup> for 7 days. Eighty-percent confluent PHH monolayers were  
189 exposed to HCVcc Jc1 infection for 3 days. FLAG peptide (100 µg/mL) or cell culture  
190 supernatants from mock electroporated cells were used for control experiments. HCV  
191 infection was assessed by RT-qPCR of intracellular HCV RNA, immunostaining using  
192 HCV E2-specific AP33 antibody or luciferase activity as described (25, 27, 28).

193

194 ***RNA purification***

195 For total RNA purification, Huh7.5.1 cells, PHH and human liver tissues were lysed  
196 using TRI-reagent (MRC) and RNA purified either according to the manufacturer's  
197 instructions or in combination with the Direct-zol RNA MiniPrep (Zymo Research).  
198 RNA quantity and quality was assessed using NanoDrop (Thermo Scientific) and  
199 Bioanalyzer 2100 (Illumina) with a quality cut-off of RNA Integrity Number >8. HCV

200 RNA was purified from cell supernatants using the QIAamp® Viral RNA Mini kit  
201 (Qiagen) according to manufacturer's instructions.

202

### 203 ***Small RNA library preparation and deep sequencing***

204 The preparation and sequencing of small RNA libraries were performed by the  
205 IGBMC Microarray and Sequencing Platform (Strasbourg, France) as described (29).

206 Libraries were prepared using 1.2 µg of total RNA, which was processed using the  
207 TruSeq RNA Sample Prep Kit according to the Illumina protocol. Large-scale small  
208 RNA-Seq was performed using an Illumina HiSeq 2500 instrument with a read length  
209 of 50 nt.

210

### 211 ***Reverse Transcription Real-Time quantitative PCR (RT-qPCR)***

212 Quantitative real-time PCRs were established as described (30) using a Corbett  
213 Rotor-gene 6000 Real-Time PCR System (Qiagen). For mature miRNA analysis, total  
214 RNA (100 ng) was first polyadenylated and reverse transcribed using the miScript II  
215 RT system (Qiagen) according to the manufacturer's instructions. The obtained  
216 cDNA (2 µl of a 10<sup>-1</sup> dilution) was subject to RT-qPCR using the miScript SYBR  
217 Green PCR kit (Qiagen). Primers were the mature miRNA sequence for the forward  
218 primers (as indicated at the Sanger miRBase database, v19.0 (31)), and the  
219 universal miScript primer (Qiagen) for the reverse primer. To check for RT-qPCR  
220 efficiency, standard curves were performed using 10-fold dilution series of total RNA  
221 from naive Huh7.5.1 cells. Data were analyzed using the  $\Delta\Delta C_t$  method using small  
222 nucleolar RNA, C/D box 61 (SNORD61) as an endogenous reference, and the non-  
223 infected samples as a calibrator (32).

224

225 ***miRNA transfection***

226 Reverse transfection was performed using RNAiMax reagent according to the  
227 manufacturer's instructions (Life Technologies). Unless otherwise indicated, all  
228 siRNAs and miRNA mimics were used at a concentration of 20 nM while anti-  
229 miRNAs were used at a concentration of 100 nM.

230

231 ***Small molecule inhibitor and DAA treatments***

232 To inhibit nuclear factor kappa B (NF- $\kappa$ B) signaling, control or miR-146a-5p-  
233 transfected differentiated Huh7 or Huh7.5.1 cells were incubated in the presence or  
234 the absence of 6.25  $\mu$ M ACHP for 24h. Subsequently, cells were infected using  
235 HCVcc (Jc1) for 5 days, lysed and RNA purified for miRNA expression analysis. Non-  
236 infected cells were analyzed in parallel as controls. This concentration of ACHP was  
237 not cytotoxic in Huh7.5.1 cells as assed using Presto Blue reagent according to  
238 manufacturer's recommendations (Life Technologies). To counteract HCV infection *in*  
239 *vitro*, differentiated Huh7.5.1 cells were infected with HCVcc (Jc1E2<sup>FLAG</sup>) for 7 days  
240 and subsequently treated for 4 weeks using a cocktail of 5 nM DCV, 1  $\mu$ M SOF and  
241 0.5  $\mu$ M SMV. After two additional weeks of washout, HCV RNA load and miR-146a-  
242 5p expression were assessed by RT-qPCR in cell supernatants and cell lysates,  
243 respectively, as described above. HCV-infected untreated cells were analyzed in  
244 parallel as controls. Cell culture media containing or not DAAs were changed three  
245 times per week.

246

247 ***Analysis of cell proliferation and cell cycle***

248 Differentiated Huh7.5.1 cells were reverse transfected with non-targeting control,  
249 miR-146a-5p mimic or siSTAT3 as described above. Twenty-four, 48, 72, and 96h

250 post-transfection, cells were detached and cell proliferation was assessed by cell  
251 counting using a BioRad TC20 automated cell counter (BioRad). To analyze the cell  
252 cycle, cells were fixed 24, 48, 72, and 96h post-transfection in cold 70% ethanol for  
253 30 min and DNA staining was performed for 30 min at 37 °C using 50 µg mL<sup>-1</sup>  
254 propidium iodide (Sigma Aldrich) and 0.1 mg mL<sup>-1</sup> RNase A (Sigma Aldrich) in PBS.  
255 Samples were acquired on a FACScan flow cytometer with doublet discrimination  
256 module on FL3 (Becton Dickinson).

257

### 258 ***Microarray***

259 Genome-wide mRNA profiling in differentiated hepatocyte-like Huh7.5.1 cells over-  
260 expressing miR-146a-5p was performed using GeneChip Human Gene 1.0 ST array  
261 (Affymetrix TSA) at the IGBMC Microarray and Sequencing Platform (Illkirch,  
262 France). Briefly, biotinylated single strand cDNA targets were prepared as described  
263 (33). Following fragmentation and end-labelling, hybridization of 2.07 µg of cDNAs  
264 was performed using the GeneChip® Fluidics Station 450 (Affymetrix) for 16h at  
265 45°C. The array strips were imaged using the GeneChip® Scanner 3000 7G  
266 (Affymetrix) at a resolution of 0.7 µm. Three biological replicates were run for each  
267 condition.

268

### 269 ***Effect of miR-146a on the HCV life cycle***

270 To assess the impact of miR-146a on the viral life cycle, Huh7.5.1 were transfected  
271 with miR-146a-5p mimic, anti-miR-122 or non-targeting control as described above.  
272 siCD81, anti-miR-122, and siApoE were used as controls to inhibit HCV entry,  
273 translation/replication, and assembly, respectively, and miR-122 mimic was used to  
274 promote HCV translation/replication (5, 22, 34, 35). To test the involvement of miR-

275 146a-5p in HCV entry, cells were incubated with HCVpp 48h post-transfection. HCV  
276 entry was assessed by measuring intracellular luciferase activity 72h later as  
277 described (19, 22). To study the effect of miR-146a-5p on HCV translation, cells were  
278 transfected with the indicated siRNAs, miRNAs and anti-miRNAs, and 48h later with  
279 HCV RNA (JcR2a) bearing a Renilla luciferase reporter gene sequence. HCV RNA  
280 translation was assessed by measuring intracellular luciferase activity after 4h (25,  
281 28, 36). To assess the relevance of miR-146a-5p for viral replication, cells were  
282 electroporated with JFH1/ $\Delta$ E1E2 RNA carrying a firefly luciferase reporter gene (23).  
283 HCV replicating cells were transfected 48h post-electroporation, and HCV replication  
284 was assessed by measuring intracellular firefly luciferase activity 48h later.  
285 Luciferase activity data were normalized to protein amounts, which were determined  
286 in the same lysate using DC protein Assay (BioRad) according to the manufacturer's  
287 instructions. To assess the effect of miR-146a-5p on HCV assembly/egress and  
288 infectivity, cells were transfected 48h prior to infection with HCVcc (Jc1) for 4h.  
289 HCVcc were then removed and cells incubated with complete medium for 48h. Cells  
290 were lysed to determine intracellular HCV RNA and infectivity titers as described (26,  
291 37). Extracellular HCV RNA and infectivity titers were analyzed in cell culture  
292 supernatants as described (26, 37). Specific infectivity was estimated as the ratio of  
293 TCID<sub>50</sub>/HCV RNA as described (28).

294

### 295 ***Bioinformatic and statistical analyses***

296 Processing and annotation of small RNA sequences have been described (20).  
297 Briefly, sequencing reads were preprocessed using FASTX\_Toolkit  
298 ([http://hannonlab.cshl.edu/fastx\\_toolkit](http://hannonlab.cshl.edu/fastx_toolkit)). Reads of 15 to 40 nt in length were then  
299 mapped to the human genome (assembly version hg19 – UCSC repository) using

300 Bowtie v0.12.8(38). Small RNAs were annotated and quantified using ncPRO-seq  
301 software version 1.5.1 (39), which uses the miRBase release 20 and Rfam v.11.  
302 miRNA measures were normalized using the DESeq2 software (40). Only miRNAs  
303 present in at least one of the libraries with a minimum of 10 reads were kept for  
304 further analysis of differential miRNA expression, which was performed using the  
305 DESeq2 software (40).

306 Raw data (CEL Intensity files) from genome-wide mRNA profiling were  
307 extracted from the scanned images using the Affymetrix GeneChip® Command  
308 Console (AGCC) version 4.0. CEL files were further processed with Affymetrix  
309 Expression Console software version 1.3.1 to calculate probe set signal intensities  
310 using Robust Multi-array Average (RMA) algorithms with default settings.  
311 Differentially expressed genes were selected using the FCROS method (41) setting  
312 selection error at 0.03. Functional annotation and gene network analyses of  
313 differentially regulated genes was performed by using Ingenuity Pathway Analysis  
314 (IPA Qiagen) software. In parallel, modulation of molecular pathway under miR-146a-  
315 5p over-expression was determined in Molecular Signature Database (MSigDB,  
316 ver.4.0) (42) using Gene Set Enrichment Analysis (GSEA, (43)).

317 miRNA targeting analyses were performed using MiRSystem (44), which  
318 allows retrieval of both experimentally validated and predicted miRNA targets.

319 Statistical analyses were performed using the GraphPad Prism v.6 package.  
320 The normality of dataset distribution was assessed using the D'Agostino and Pearson  
321 omnibus and the Shapiro-Wilk normality tests. Datasets with normal distribution are  
322 presented as means  $\pm$  s.d. and were analyzed by unpaired t-test with Welch's  
323 correction or one-way ANOVA as indicated in the figure legends. All other datasets  
324 are presented as medians with upper and lower quartiles and analyzed using the

325 non-parametric two-tailed Mann-Whitney test or Kruskal-Wallis test as indicated in  
326 the figure legends.

327

328 ***Gene Expression Omnibus accession numbers***

329 Genome-wide mRNA and small RNA data reported in this paper were submitted to  
330 the Gene Expression Omnibus database (GSE79341).

331 **Results**

332 ***Persistent HCV infection induces the up-regulation of miR-146a-5p in***  
333 ***hepatocytes***

334 To systematically identify HCV-induced alteration of miRNA profiles in hepatocytes,  
335 we induced a poor proliferative state as well as expression of hepatocyte-specific  
336 genes in Huh7.5.1 cells, a state-of-the-art permissive cell line for HCV infection using  
337 1% DMSO (14-16). These hepatocyte-like cells were then subjected to HCVcc (strain  
338 Jc1) infection for 7 days (20, 36) using highly purified virus particles in order to avoid  
339 any interference due to serum components or cytokines present in the cell culture  
340 medium. HCV-infection of hepatocyte-like cells resulted in the establishment of  
341 pervasive infection as assessed by immunofluorescence staining against the viral  
342 antigen E2 (Fig. 1A). We then performed high-throughput small RNA cloning and  
343 deep sequencing of these persistently HCV-infected hepatocyte-like cells (20, 45). In  
344 total, 109,543,844 reads were generated for both cells at 7 days post-infection (dpi)  
345 and non-infected controls. About 85% of total reads could be mapped to the human  
346 genome, and categorized into RNA classes based on sequence annotation (data not  
347 shown). The large majority of reads from both HCV-infected and non-infected cells  
348 were annotated as mature miRNAs of about 22 nt in length. Interestingly, infected  
349 cells presented a slight increase in the number of reads annotated as rRNA as  
350 compared to controls (data not shown). This is consistent with previous evidence of  
351 deregulated rRNA transcription in HCV-infected cultured liver cells (46). Profiling  
352 analyses indicated that HCV infection differentially regulated the expression of 72  
353 miRNAs, of which 56 were up-regulated by at least 2-fold and 16 were down-  
354 regulated 2-fold or more (Fig. 1B). Among the up-regulated miRNAs, miR-21-5p was  
355 previously reported to be enhanced by HCV in both Huh7-derived cells and in liver

356 tissues (47-49). Interestingly, miR-21-5p appears to be highly expressed in HCC  
357 tumors and cell lines where it was shown to enhance cell proliferation, migration, and  
358 invasion (50, 51). Aiming to identify additional virus-mediated alterations of miRNA  
359 patterns that may be linked to liver disease and hepatocarcinogenesis, we chose to  
360 focus our investigation on those miRNAs that were previously described to target  
361 genes associated with inflammation, fibrosis and cancer development, but have not  
362 yet been strongly linked to HCV-mediated hepatocyte injury (Table 2). By RT-qPCR  
363 we independently validated the expression of miR-146a-5p and miR-143-3p in  
364 chronically infected hepatocyte-like cells along with that of miR-21-5p, which was  
365 assessed as a positive control. Similarly to RNA-Seq, a significant increase of these  
366 miRNAs was observed upon viral infection (Fig. 1C,  $p$ -value = 0.00094, 0.00094 and  
367 0.014, respectively, two-tailed Mann-Whitney test). To better understand the link  
368 between HCV and miRNA deregulation in the liver, we further studied the modulation  
369 of these three miRNAs by HCV in primary human hepatocytes (PHH), a model that  
370 most closely reflects the *in vivo* situation. In PHH cultures that were subject to HCVcc  
371 (Jc1) infection, miR-21-5p, miR-146a-5p and miR-143-3p were significantly up-  
372 regulated (Fig. 1D,  $p$ -value = 0.002, 0.005 and 0.03, respectively, two-tailed Mann-  
373 Whitney test), confirming that the HCV-mediated enhancement of miR-21-5p, miR-  
374 146a-5p and miR-143-3p occurs in human hepatocytes. Interestingly, miR-146a-5p,  
375 which is a well-known immunoregulatory miRNA (54) was described to be up-  
376 regulated in the serum and peripheral blood mononuclear cells (PBMC) of HCV-  
377 infected patients (55, 56). Moreover, a recent piece of evidence points to an  
378 involvement of miR-146a in liver fibrosis in mice and humans independently of HCV  
379 (57). To gain insights into the clinical relevance of our findings, we studied miR-146a-  
380 5p expression in liver biopsies from chronically HCV-infected patients and HCV

381 negative individuals (Table 1). Consistently with our *in vitro* data, up-regulated miR-  
382 146a-5p was observed in HCV-positive liver tissues (Fig. 1E,  $p$ -value<0.0001, two-  
383 tailed Mann-Whitney test).

384

### 385 ***HCV-induced up-regulation of miR-146a-5p is dependent on NF- $\kappa$ B signaling***

386 Next, we investigated the molecular mechanisms by which HCV induces the  
387 expression of miR-146a-5p in hepatocytes. Previous evidence revealed that  
388 inflammation and virus infection can trigger the induction of miR-146a through  
389 activation of NF- $\kappa$ B in monocytes, lymphocytes and epithelial cells (58, 59). Since  
390 HCV infection was shown to impact on NF- $\kappa$ B signaling (60), we investigated whether  
391 the HCV-mediated induction of miR-146a-5p could be regulated by the NF- $\kappa$ B  
392 pathway. We used a specific inhibitor of the I $\kappa$ B kinase (IKK), ACHP, which prevents  
393 NF- $\kappa$ B DNA binding (61), to perturb NF- $\kappa$ B signaling in hepatocyte-like cells  
394 subjected or not to HCV infection. The efficacy of NF- $\kappa$ B inhibition was confirmed by  
395 the markedly reduced expression of miR-146a-5p in ACHP-treated non-infected cells  
396 (Fig. 1F). Cells infected in the presence of the NF- $\kappa$ B inhibitor, at a concentration that  
397 did not affect cell viability, displayed a significant decrease in miR-146a-5p  
398 expression as compared to control infected cells (Fig. 1F,  $p$ -value < 0.0001),  
399 indicating that the HCV-induced miR-146a-5p expression is NF- $\kappa$ B dependent. To  
400 test whether retinoic acid-inducible gene-I (RIG-I), which is a known regulator of NF-  
401  $\kappa$ B activity (62), could be involved in this process, we analyzed HCV-induced miR-  
402 146a-5p expression in Huh7 cells - which exhibit functional RIG-I signaling in contrast  
403 to Huh7.5.1 cells - in the presence and absence of the NF- $\kappa$ B inhibitor. As we  
404 observed comparable inhibition of HCV-induced miR-146a-5p expression between  
405 hepatocyte-like Huh7.5.1 and hepatocyte-like Huh7 cells using the NF- $\kappa$ B inhibitor,

406 the RIG-I signaling does not appear to play a major role in this process (data not  
407 shown). Collectively, these data indicate that NF- $\kappa$ B signaling regulates miR-146a-5p  
408 expression in HCV-infected hepatocytes.

409

410 ***miR-146a-5p regulates cell metabolism and pathways that contribute to***  
411 ***pathogenesis of liver disease***

412 We then sought to explore the functional relevance of miR-146a-5p up-regulation in  
413 hepatocytes. As miR-146a is well known to enhance cell proliferation in PBMC, we  
414 evaluated whether this miRNA promotes cell proliferation and cell cycle progression  
415 in hepatocyte-like cells. siRNA targeting *STAT3* was used as a control to inhibit  
416 proliferation of hepatocyte-like cells (63). In contrast to cells silenced for *STAT3*,  
417 which displayed decreased cell proliferation over time, cells over-expressing miR-  
418 146a-5p did not show any significant alteration of cell proliferation within 96h of  
419 transfection as compared to control-transfected cells (Fig. 2A). To confirm this  
420 finding, we analyzed the cell cycle distribution of hepatocyte-like cells upon miR-  
421 146a-5p transfection by flow cytometry. While silencing of *STAT3* resulted in  
422 markedly slower percentages of cells in S and G2/M phases, over-expressing miR-  
423 146a-5p did not impact on the overall cell cycle distribution (Fig. 2B). Taken together,  
424 these data suggest that miR-146a-5p does not promote cell proliferation of  
425 hepatocyte-like cells.

426 To investigate the pathways regulated by miR-146a-5p in our model in an unbiased  
427 manner we performed a genome-wide transcriptomic analysis of hepatocyte-like cells  
428 upon miR-146a-5p over-expression (Fig. 3). By RT-qPCR we assessed a consistent  
429 increase of miR-146a-5p upon miRNA transfection prior to genome-wide microarray  
430 analysis (data not shown). As compared to control cells, enhanced miR-146a-5p

431 expression in hepatocyte-like cells resulted in a significant deregulation of 274 genes,  
432 including 63 up-regulated and 211 down-regulated genes (Fig. 3A,  $p$ -value < 0.01,  
433 FCROS method). Interestingly, *interleukin-1 receptor-associated kinase 1 (IRAK1)*  
434 and the chemokine *C-X-C motif chemokine ligand 8 (CXCL8)*, two known targets of  
435 miR-146a-5p, were among the down-regulated genes. In line with a previously shown  
436 implication of miR-146a-5p and *IRAK1* in inflammatory responses in immune cells  
437 (54), our data suggest a role of miR-146a-5p in inflammation signaling in hepatocyte-  
438 like cells. Functional annotation using the IPA systems biology tool further showed an  
439 involvement of miR-146a-5p in gene networks related to inflammatory response, cell  
440 death and survival, cell-to-cell signaling and interaction as well as cancer-associated  
441 processes (data not shown). Moreover, when running all the significantly deregulated  
442 genes through Ingenuity's *Tox Function* prediction, the top toxicological functions that  
443 were most strongly associated with miR-146a-5p over-expression were related to  
444 liver disease including liver inflammation and hepatitis, glutathione depletion - a  
445 process associated with liver disease progression, liver damage, cholestasis,  
446 cirrhosis and necrosis (Fig. 3B). Together with previous evidence linking miR-146a  
447 deregulation to liver fibrosis (57), this piece of data suggests that the modulation of  
448 miR-146a-5p expression may contribute to liver disease pathogenesis. To gain  
449 further insights into the role of miR-146a-5p in hepatocyte injury and progression of  
450 liver disease, we chose to extend our computational analysis of miR-146a-5p over-  
451 expressing cells by retrieving those gene sets that shared common regulation by  
452 miR-146a-5p through GSEA (43). In contrast to control-transfected hepatocyte-like  
453 cells, miR-146a-5p over-expressing cells presented a gene profile underlying strong  
454 repression of inflammatory and immune response pathways along with an  
455 enrichment of defined metabolic regulatory networks, such as regulation of fatty acid

456 metabolism and energetic metabolism (Fig. 3C). In particular, miR-146a-5p over-  
457 expression resulted in repression of oxidative phosphorylation while it enhanced  
458 pyruvate metabolism and citrate cycle (Fig. 3C), suggesting an induction of metabolic  
459 changes similar to those observed in tumor cells (64). Overall, our transcriptomic  
460 profiling indicates an involvement of miR-146a-5p in gene networks that are  
461 associated with liver disease and HCC development. Given that antiviral therapy  
462 leading to HCV cure does not eliminate the risk of hepatitis C patients to develop  
463 HCC (2), we sought to determine the expression of miR-146a-5p in chronically HCV-  
464 infected hepatocyte-like cells treated with a state-of-the-art combination of DAAs.  
465 The DAA-treatment, which decreased the viral load in cell supernatants to the limit of  
466 quantification of the RT-qPCR assay, did not restore the HCV-mediated over-  
467 expression of miR-146a-5p to its level in non-infected control cells (Fig. 4). These  
468 results suggest that the over-expression of miR-146a, which is induced by HCV  
469 infection and is not reversed by antiviral therapy may contribute to maintain the  
470 increased risk of HCC development in patients cured from hepatitis C.

471 Since the up-regulation of miR-146a-5p results in the enhancement of fatty acid  
472 metabolism, which is instrumental to HCV replication, this piece of data suggests that  
473 in addition to modulating pathways associated with liver disease pathogenesis, miR-  
474 146a-5p may fine-tune the metabolic activity of hepatocytes upon viral infection, and  
475 eventually act on the viral replication cycle itself.

476

477 ***miR-146a-5p promotes the production of infectious HCV particles without***  
478 ***affecting viral entry or replication***

479 To assess the potential impact of miR-146a-5p on the HCV life cycle, we performed a  
480 series of gain-of-function and loss-of-function experiments using HCVpp,

481 HCV/ $\Delta$ E1E2 RNA and HCVcc to investigate the role of miR-146a-5p in HCV entry,  
482 translation, replication, assembly and infectivity. Loss-of-function perturbation of  
483 essential HCV host factors required either for viral entry, viral translation/replication,  
484 or viral assembly using siCD81, anti-miR-122, or siApoE, respectively, were used as  
485 controls. miR-122 mimic was used as a gain-of-function control in  
486 translation/replication studies. To study the impact of miR-146a-5p on viral entry,  
487 Huh7.5.1 cells were first transfected with siRNAs, miR-146a-5p mimic or anti-miR-  
488 146a and then incubated with luciferase-reporter HCVpp or VSVpp, which were used  
489 as an unrelated control virus. In contrast to the silencing of *CD81*, which resulted in a  
490 dramatic decrease in HCVpp entry, modulating the expression of miR-146a-5p did  
491 not significantly affect this process (Fig. 5A). VSVpp entry was neither affected by the  
492 modulation of miR-146a-5p expression (data not shown). To assess the impact of  
493 miR-146a-5p on translation and replication, we used a Renilla luciferase reporter  
494 HCV genome (JcR2a) and a firefly luciferase reporter assembly-deficient HCV RNA  
495 (JFH1/ $\Delta$ E1E2). The former was transfected into Huh7.5.1 cells, which had previously  
496 been transfected with siRNA, miRNA or anti-miRNA, while the latter was  
497 electroporated into cells prior to siRNA/miRNA transfection. In contrast to miR-122  
498 and anti-miR-122, which significantly increased and decreased both HCV translation  
499 and replication, respectively, miR-146a-5p and anti-miR-146a did not significantly  
500 affect HCV replication although being able to modulate HCV translation when this  
501 step was studied independently of viral replication (Fig. 5B-C). Finally, to test whether  
502 miR-146a-5p may play a role in HCV assembly, we measured HCV RNA and viral  
503 infectivity in both lysates and supernatants of Huh7.5.1 cells that were infected with  
504 HCVcc (Jc1) following transfection of siRNA, miRNA or anti-miRNA. In contrast to  
505 cells with silenced *apoE*, in which viral assembly was significantly impaired, over-

506 expression of miR-146a-5p increased both extracellular and intracellular viral  
507 infectivity (Fig. 5D-E, p-value = 0.005 and 0.036, respectively). In contrast, the anti-  
508 miR-146a had no significant effect on viral infectivity (Fig. 5D-E, p-value = 0.7 and  
509 0.08, respectively). Since the specific infectivity (as assessed by the ratio  
510 TCID<sub>50</sub>/HCV RNA) of the viral particles was not significantly affected by the  
511 modulation of the expression of miR-146a-5p (data not shown), these results suggest  
512 that miR-146a-5p promotes HCV assembly and particle release without increasing  
513 the specific infectivity of the produced virions. Taken together, we revealed that  
514 ectopic miR-146a-5p expression promoted late steps of the HCV replication cycle,  
515 likely by increasing HCV assembly/egress (Fig. 5A-E). However, miR-146a-5p did  
516 not appear to be essential for HCV morphogenesis since anti-miR-146a did not  
517 inhibit the production of infectious viral particles (Fig. 5D-E). These results uncover  
518 miR-146a-5p as a new pro-viral host factor for HCV infection that increases the  
519 production of infectious viral particles.

520 Collectively, our data indicate that the HCV-induced increase in miR-146a-5p  
521 expression promotes both virus infection and metabolic pathways associated with  
522 liver disease pathogenesis.

523

## 524 **Discussion**

525 Progression of chronic hepatitis C to poor prognosis liver disease and HCC is a  
526 multifactorial process that involves persistent hepatic inflammation, progressive liver  
527 fibrogenesis, development of neoplastic clones and finally establishment of a  
528 carcinogenic tissue microenvironment (65). Being central players in both  
529 physiological and pathological conditions, miRNAs most likely contribute to HCV-  
530 driven liver disease (3, 8). Moreover, increasing evidence points to a role of miRNAs

531 in fine-tuning HCV-hepatocyte interactions (4, 8). However, the lack of efficient and  
532 convenient model systems to investigate the biological circuits of virus-host  
533 interactions represents a major obstacle for the understanding of the mechanisms  
534 linking HCV infection, inflammation and carcinogenesis. By performing high-  
535 throughput small RNA-Seq and computational analyses in a hepatocyte-like based  
536 model system, which enables persistent HCV infection (14-16) we identified 72  
537 miRNAs significantly modulated by HCV that could have a putative involvement in  
538 virus-driven liver disease and HCC (Fig. 1, Table 2). Indeed, 20 out of these 72  
539 miRNAs were already known for their implication in inflammation, fibrosis and cancer  
540 development. This subset of miRNAs included: miR-122, which is a key player in  
541 HCV infection and liver disease (reviewed in (4)); miR-21-5p, which has been  
542 consistently shown to be implicated in HCV infection and liver disease (47-49) and  
543 miR-146a-5p, a well-known immunoregulatory miRNA further described to be  
544 associated with liver fibrosis and HCC (56, 66-68). Moreover, members of the miR-27  
545 family of miRNAs, which contribute to the regulation of the lipid metabolism, have  
546 recently been reported to be increased by HCV and to contribute to liver steatosis  
547 (52, 53).

548 By pursuing our investigation in PHH and clinical liver tissues from HCV-  
549 infected patients (Fig. 1), we provided first evidence that HCV induces up-regulation  
550 of miR-146a-5p in hepatocytes. Interestingly, miR-146a has been previously  
551 associated with HCV infection: an increased expression of this miRNA was observed  
552 in the serum and PBMC of HCV-infected patients, suggesting a role of circulating  
553 miR-146-5p as a biomarker for hepatic injury (55, 56). In line with this, hepatitis B  
554 virus (HBV) has also been shown to increase miR-146a in human hepatoma cell  
555 lines and chronically HBV-infected patient-derived liver tissues (69). However, the

556 cross-talk between miR-146a-5p and HCV and its relevance for hepatocyte injury has  
557 not yet been evidenced. Taking advantage of a series of well established functional  
558 assays to investigate distinct steps of virus-host interactions, we discovered that miR-  
559 146a-5p exerts a pro-viral effect in liver cells likely by modulating HCV  
560 assembly/egress (Fig. 5D-E). In contrast to data reported with HepG2 cells where a  
561 high ectopic expression of miR-146a was shown to target *epidermal growth factor*  
562 *receptor (EGFR)* (70), which is a HCV entry co-factor in liver cells (22), ectopic  
563 expression of miR-146a-5p in our experimental conditions did not affect *EGFR*  
564 expression (data not shown) in line with the absent modulation of the early steps of  
565 HCV infection upon miR-146a-5p over-expression (Fig. 5A). Collectively, our data  
566 uncover miR-146a-5p as a new pro-viral host factor for HCV infection. By over-  
567 expressing miR-146a-5p in liver cells we observed its involvement in key metabolic  
568 pathways, including proteasome pathway and fatty acid metabolism (Fig. 3C), which  
569 in turn were associated with HCV assembly (71-73). Moreover, we observed that  
570 miR-146a-5p likely modulates the anaerobic energetic metabolism in hepatocyte-like  
571 cells (Fig. 3). Since HCV has been shown to enhance cellular glucose consumption  
572 (74), miR-146a-5p may be implicated in the HCV-induced aerobic glycolysis shift that  
573 is also a hallmark of tumor cells. This piece of data suggests that by regulating liver  
574 cell metabolism, miR-146a-5p may be beneficial for HCV infection and potentially  
575 play a role in HCV-driven liver disease.

576         Beyond cell metabolism, our pathway enrichment analysis further suggests a  
577 pivotal role of miR-146a in down-regulating inflammation signaling and immune  
578 responses in hepatocytes (Fig. 3). This is consistent with recent evidence that  
579 miR146a contributes to the escape of HCC cells from anti-tumor immune responses  
580 *in vivo* (67). In the context of HCV infection, up-regulation of miR-146a-5p may

581 enable HCV-infected cells to escape from immune surveillance mechanisms,  
582 facilitating the maintenance of infection. Noteworthy, our pathway analysis also  
583 highlighted a role of miR-146a-5p in promoting liver inflammation and disease  
584 progression (Fig. 3). Indeed, miR-146a was recently described as involved in an  
585 inflammatory feedback circuit regulating the cross-talk between hepatocytes and  
586 human stellate cells (HSC) (57). In rat models of liver fibrosis, cytokines were shown  
587 to increase the expression of both miR-146a and miR-21 that in turn sustain  
588 repression of hepatocyte nuclear factor 1a (HNF1a) in hepatocytes, thus enhancing  
589 hepatocellular inflammation, cytokine release, activation of HSC and disease  
590 progression (57). This is also in line with previous studies showing up-regulation of  
591 miR-146a in the plasma of mice, which were subject to liver inflammation induced by  
592 cytidine-phosphate-guanosine (CpG) motif and lipopolysaccharide (LPS) (55).  
593 Interestingly, the same study highlighted enhanced miR-146a expression in mice with  
594 acetaminophen-induced liver injury characterized by little inflammation (55). Given its  
595 central role in liver cell homeostasis and signaling (Fig. 3), we propose that miR-  
596 146a-5p might serve as a molecular switch that fine-tunes stress signaling in  
597 hepatocytes, enabling modulation of metabolic activity in response to micro-  
598 environmental changes. Thus impairment of miR-146a regulation and signaling may  
599 participate to hepatocellular injury. This could also provide clues about the putative  
600 modulation of miR-146a expression during the progression of liver disease. While  
601 enhanced expression of this miRNA was observed in chronic HCV infection (Fig. 1E)  
602 and fibrosis (57), its repression was associated with invasiveness of HCC tumors (56,  
603 67) thus suggesting a tumor suppressor function for miR-146a. Further investigation  
604 will be necessary to better understand the molecular mechanisms of miR-146a-  
605 mediated liver disease pathogenesis and HCC development.

606           Taken together, our study indicates a novel involvement of miR-146a-5p in  
607 promoting HCV infection and metabolic pathways associated with liver disease  
608 progression, and contributes to a better understanding of HCV-induced liver disease  
609 pathogenesis ultimately providing novel potential therapeutic targets to prevent HCC  
610 in HCV-infected patients.

611 **Funding information.** This work was supported by the European Union  
612 (INTERREG-IV-Rhin Supérieur-FEDER-Hepato-Regio-Net to M.B.Z. and T.F.B. and  
613 FP7 HepaMab to T.F.B.), ANRS (2012/239 to M.B.Z. and T.F.B., 2013/108 to T.F.B),  
614 by ARC, Paris and Institut Hospitalo-Universitaire, Strasbourg (TheraHCC IHUARC  
615 IHU201301187 to T.F.B.), Inserm, and University of Strasbourg. The IGBMC  
616 Microarray and Sequencing platform was supported by the FG National  
617 Infrastructure, funded as part of the "Investissements d'Avenir" program managed by  
618 the Agence Nationale pour la Recherche (ANR-10-INBS-0009). This work has been  
619 published under the framework of the LABEX ANR-10-LABX-0028\_HEPSYS and  
620 benefits from a funding from the state managed by the French National Research  
621 Agency as part of the Investments for the future program. S.P. and E.C. were  
622 supported by fellowships from the French Ministry of Research. The funders had no  
623 role in study design, data collection and interpretation, or the decision to submit the  
624 work for publication.

625

626 **Acknowledgments.** We thank Dr. R. Bartenschlager (University of Heidelberg,  
627 Germany) for providing the plasmid for production of HCVcc, Dr. F. Chisari (The  
628 Scripps Research Institute, La Jolla, CA) for the gift of Huh7.5.1 cells, and Dr. A.  
629 Patel (MRC Virology Unit, Glasgow, UK) for E2-specific mAb AP33. We acknowledge  
630 N. Van Renne, S. Coassolo and A. Mawa (Inserm U1110, Strasbourg, France) as  
631 well as A. Weiss, Dr. L. Brino and Dr. D. Dembele (IGBMC, Department of Functional  
632 Genomics and Cancer, Illkirch, France) for excellent technical assistance as well as  
633 helpful discussions regarding transfection protocols and computational analyses. We  
634 thank B. Campana, M.D. (Departement of Biomedicine, University Hospital Basel,  
635 Basel, Switzerland) for providing clinical information about the patients enrolled in the

636 study. We thank Dr. S. Pfeffer (IBMC, Strasbourg, France) for helpful discussions  
637 regarding miRNA expression analyses. The small RNA-Seq and microarray analyses  
638 as well as bioinformatics were performed at IGBMC Microarray and Sequencing  
639 Platform (Illkirch, France), member of the France Genomique program.

640

641 **Author contribution.** T.F.B and M.B.Z initiated the project. M.B.Z. supervised  
642 research. S.B., S.P. and M.B.Z. designed experiments. S.B., S.P., H.E.S., S.C.D.,  
643 E.C., M.A.O., J.B. and C.T. performed experiments. S.B., S.P., H.E.S., E.C., T.Y.,  
644 J.B., T.F.B. and M.B.Z. analyzed data. I.F., C.S., M.H.H. and P.P. provided essential  
645 reagents. S.B., S.P., H.E.S and I.F. designed figures and tables. S.B., S.P. and  
646 M.B.Z. wrote the paper. T.F.B edited the manuscript. All authors read and approved  
647 the manuscript. The authors declare no conflict of interest.

648 **References**

- 649 1. **Chung RT, Baumert TF.** 2014. Curing chronic hepatitis C--the arc of a  
650 medical triumph. *N Engl J Med* **370**:1576-1578.
- 651 2. **van der Meer AJ, Veldt BJ, Feld JJ, Wedemeyer H, Dufour JF, Lammert F,**  
652 **Duarte-Rojo A, Heathcote EJ, Manns MP, Kuske L, Zeuzem S, Hofmann**  
653 **WP, de Knecht RJ, Hansen BE, Janssen HL.** 2012. Association between  
654 sustained virological response and all-cause mortality among patients with  
655 chronic hepatitis C and advanced hepatic fibrosis. *JAMA* **308**:2584-2593.
- 656 3. **Szabo G, Bala S.** 2013. MicroRNAs in liver disease. *Nat Rev Gastroenterol*  
657 *Hepatol* **10**:542-552.
- 658 4. **Bandiera S, Pfeffer S, Baumert TF, Zeisel MB.** 2015. miR-122--a key factor  
659 and therapeutic target in liver disease. *J Hepatol* **62**:448-457.
- 660 5. **Jopling CL, Yi M, Lancaster AM, Lemon SM, Sarnow P.** 2005. Modulation  
661 of hepatitis C virus RNA abundance by a liver-specific MicroRNA. *Science*  
662 **309**:1577-1581.
- 663 6. **Henke JI, Goergen D, Zheng J, Song Y, Schuttler CG, Fehr C, Junemann**  
664 **C, Niepmann M.** 2008. microRNA-122 stimulates translation of hepatitis C  
665 virus RNA. *EMBO J* **27**:3300-3310.
- 666 7. **Li Y, Masaki T, Yamane D, McGivern DR, Lemon SM.** 2013. Competing and  
667 noncompeting activities of miR-122 and the 5' exonuclease Xrn1 in regulation  
668 of hepatitis C virus replication. *Proc Natl Acad Sci U S A* **110**:1881-1886.
- 669 8. **Shrivastava S, Mukherjee A, Ray RB.** 2013. Hepatitis C virus infection,  
670 microRNA and liver disease progression. *World J Hepatol* **5**:479-486.

- 671 9. **Gragnani L, Piluso A, Fognani E, Zignego AL.** 2015. MicroRNA expression  
672 in hepatitis C virus-related malignancies: A brief review. *World J Gastroenterol*  
673 **21:8562-8568.**
- 674 10. **Fan HX, Tang H.** 2014. Complex interactions between microRNAs and  
675 hepatitis B/C viruses. *World J Gastroenterol* **20:13477-13492.**
- 676 11. **Varnholt H, Drebber U, Schulze F, Wedemeyer I, Schirmacher P, Dienes**  
677 **HP, Odenthal M.** 2008. MicroRNA gene expression profile of hepatitis C virus-  
678 associated hepatocellular carcinoma. *Hepatology* **47:1223-1232.**
- 679 12. **Ura S, Honda M, Yamashita T, Ueda T, Takatori H, Nishino R, Sunakozaka**  
680 **H, Sakai Y, Horimoto K, Kaneko S.** 2009. Differential microRNA expression  
681 between hepatitis B and hepatitis C leading disease progression to  
682 hepatocellular carcinoma. *Hepatology* **49:1098-1112.**
- 683 13. **Steinmann E, Pietschmann T.** 2013. Cell culture systems for hepatitis C  
684 virus. *Curr Top Microbiol Immunol* **369:17-48.**
- 685 14. **Sainz B, Jr., Chisari FV.** 2006. Production of infectious hepatitis C virus by  
686 well-differentiated, growth-arrested human hepatoma-derived cells. *J Virol*  
687 **80:10253-10257.**
- 688 15. **Bauhofer O, Ruggieri A, Schmid B, Schirmacher P, Bartenschlager R.**  
689 2012. Persistence of HCV in quiescent hepatic cells under conditions of an  
690 interferon-induced antiviral response. *Gastroenterology* **143:429-438 e428.**
- 691 16. **Xiao F, Fofana I, Thumann C, Maily L, Alles R, Robinet E, Meyer N,**  
692 **Schaeffer M, Habersetzer F, Doffoel M, Leyssen P, Neyts J, Zeisel MB,**  
693 **Baumert TF.** 2015. Synergy of entry inhibitors with direct-acting antivirals  
694 uncovers novel combinations for prevention and treatment of hepatitis C. *Gut*  
695 **64:483-494.**

- 696 17. **Owsianka A, Tarr AW, Juttla VS, Lavillette D, Bartosch B, Cosset FL, Ball**  
697 **JK, Patel AH.** 2005. Monoclonal antibody AP33 defines a broadly neutralizing  
698 epitope on the hepatitis C virus E2 envelope glycoprotein. *J Virol* **79**:11095-  
699 11104.
- 700 18. **Zhong J, Gastaminza P, Cheng G, Kapadia S, Kato T, Burton DR, Wieland**  
701 **SF, Uprichard SL, Wakita T, Chisari FV.** 2005. Robust hepatitis C virus  
702 infection in vitro. *Proc Natl Acad Sci U S A* **102**:9294-9299.
- 703 19. **Krieger SE, Zeisel MB, Davis C, Thumann C, Harris HJ, Schnober EK,**  
704 **Mee C, Soulier E, Royer C, Lambotin M, Grunert F, Dao Thi VL, Dreux M,**  
705 **Cosset FL, McKeating JA, Schuster C, Baumert TF.** 2010. Inhibition of  
706 hepatitis C virus infection by anti-claudin-1 antibodies is mediated by  
707 neutralization of E2-CD81-claudin-1 associations. *Hepatology* **51**:1144-1157.
- 708 20. **Maily L, Xiao F, Lupberger J, Wilson GK, Aubert P, Duong FH, Calabrese**  
709 **D, Leboeuf C, Fofana I, Thumann C, Bandiera S, Lutgehetmann M, Volz T,**  
710 **Davis C, Harris HJ, Mee CJ, Girardi E, Chane-Woon-Ming B, Ericsson M,**  
711 **Fletcher N, Bartenschlager R, Pessaux P, Vercauteren K, Meuleman P,**  
712 **Villa P, Kaderali L, Pfeffer S, Heim MH, Neunlist M, Zeisel MB, Dandri M,**  
713 **McKeating JA, Robinet E, Baumert TF.** 2015. Clearance of persistent  
714 hepatitis C virus infection in humanized mice using a claudin-1-targeting  
715 monoclonal antibody. *Nat Biotechnol* **33**:549-554.
- 716 21. **Bartosch B, Dubuisson J, Cosset FL.** 2003. Infectious hepatitis C virus  
717 pseudo-particles containing functional E1-E2 envelope protein complexes. *J*  
718 *Exp Med* **197**:633-642.
- 719 22. **Lupberger J, Zeisel MB, Xiao F, Thumann C, Fofana I, Zona L, Davis C,**  
720 **Mee CJ, Turek M, Gorke S, Royer C, Fischer B, Zahid MN, Lavillette D,**

- 721 **Fresquet J, Cosset FL, Rothenberg SM, Pietschmann T, Patel AH,**  
722 **Pessaux P, Doffoel M, Raffelsberger W, Poch O, McKeating JA, Brino L,**  
723 **Baumert TF.** 2011. EGFR and EphA2 are host factors for hepatitis C virus  
724 entry and possible targets for antiviral therapy. *Nat Med* **17**:589-595.
- 725 23. **Wakita T, Pietschmann T, Kato T, Date T, Miyamoto M, Zhao Z, Murthy K,**  
726 **Habermann A, Krausslich HG, Mizokami M, Bartenschlager R, Liang TJ.**  
727 2005. Production of infectious hepatitis C virus in tissue culture from a cloned  
728 viral genome. *Nat Med* **11**:791-796.
- 729 24. **Merz A, Long G, Hiet MS, Brugger B, Chlanda P, Andre P, Wieland F,**  
730 **Krijnse-Locker J, Bartenschlager R.** 2011. Biochemical and morphological  
731 properties of hepatitis C virus particles and determination of their lipidome. *J*  
732 *Biol Chem* **286**:3018-3032.
- 733 25. **Reiss S, Rebhan I, Backes P, Romero-Brey I, Erfle H, Matula P, Kaderali**  
734 **L, Poenisch M, Blankenburg H, Hiet MS, Longrich T, Diehl S, Ramirez F,**  
735 **Balla T, Rohr K, Kaul A, Buhler S, Pepperkok R, Lengauer T, Albrecht M,**  
736 **Eils R, Schirmacher P, Lohmann V, Bartenschlager R.** 2011. Recruitment  
737 and activation of a lipid kinase by hepatitis C virus NS5A is essential for  
738 integrity of the membranous replication compartment. *Cell Host Microbe* **9**:32-  
739 45.
- 740 26. **Lindenbach BD, Evans MJ, Syder AJ, Wolk B, Tellinghuisen TL, Liu CC,**  
741 **Maruyama T, Hynes RO, Burton DR, McKeating JA, Rice CM.** 2005.  
742 Complete replication of hepatitis C virus in cell culture. *Science* **309**:623-626.
- 743 27. **Fofana I, Krieger SE, Grunert F, Glauben S, Xiao F, Fafi-Kremer S, Soulier**  
744 **E, Royer C, Thumann C, Mee CJ, McKeating JA, Dragic T, Pessaux P,**  
745 **Stoll-Keller F, Schuster C, Thompson J, Baumert TF.** 2010. Monoclonal

- 746 anti-claudin 1 antibodies prevent hepatitis C virus infection of primary human  
747 hepatocytes. *Gastroenterology* **139**:953-964, 964 e951-954.
- 748 28. **Da Costa D, Turek M, Felmler DJ, Girardi E, Pfeffer S, Long G,**  
749 **Bartenschlager R, Zeisel MB, Baumert TF.** 2012. Reconstitution of the  
750 entire hepatitis C virus life cycle in nonhepatic cells. *J Virol* **86**:11919-11925.
- 751 29. **Mobuchon L, Marthey S, Le Guillou S, Laloe D, Le Provost F, Leroux C.**  
752 2015. Food Deprivation Affects the miRNome in the Lactating Goat Mammary  
753 Gland. *PLoS one* **10**:e0140111.
- 754 30. **Buck AH, Perot J, Chisholm MA, Kumar DS, Tuddenham L, Cognat V,**  
755 **Marcinowski L, Dolken L, Pfeffer S.** 2010. Post-transcriptional regulation of  
756 miR-27 in murine cytomegalovirus infection. *RNA* **16**:307-315.
- 757 31. **Griffiths-Jones S.** 2004. The microRNA Registry. *Nucleic Acids Res*  
758 **32**:D109-111.
- 759 32. **Schmittgen TD, Livak KJ.** 2008. Analyzing real-time PCR data by the  
760 comparative C(T) method. *Nat Protoc* **3**:1101-1108.
- 761 33. **Adamo A, Atashpaz S, Germain PL, Zanella M, D'Agostino G, Albertin V,**  
762 **Chenoweth J, Micale L, Fusco C, Unger C, Augello B, Palumbo O,**  
763 **Hamilton B, Carella M, Donti E, Pruneri G, Selicorni A, Biamino E,**  
764 **Prontera P, McKay R, Merla G, Testa G.** 2015. 7q11.23 dosage-dependent  
765 dysregulation in human pluripotent stem cells affects transcriptional programs  
766 in disease-relevant lineages. *Nat Genet* **47**:132-141.
- 767 34. **Li Q, Brass AL, Ng A, Hu Z, Xavier RJ, Liang TJ, Elledge SJ.** 2009. A  
768 genome-wide genetic screen for host factors required for hepatitis C virus  
769 propagation. *Proc Natl Acad Sci U S A* **106**:16410-16415.

- 770 35. **Benga WJ, Krieger SE, Dimitrova M, Zeisel MB, Parnot M, Lupberger J,**  
771 **Hildt E, Luo G, McLauchlan J, Baumert TF, Schuster C.** 2010.  
772 Apolipoprotein E interacts with hepatitis C virus nonstructural protein 5A and  
773 determines assembly of infectious particles. *Hepatology* **51**:43-53.
- 774 36. **Pietschmann T, Kaul A, Koutsoudakis G, Shavinskaya A, Kallis S,**  
775 **Steinmann E, Abid K, Negro F, Dreux M, Cosset FL, Bartenschlager R.**  
776 2006. Construction and characterization of infectious intragenotypic and  
777 intergenotypic hepatitis C virus chimeras. *Proc Natl Acad Sci U S A* **103**:7408-  
778 7413.
- 779 37. **Gastaminza P, Kapadia SB, Chisari FV.** 2006. Differential biophysical  
780 properties of infectious intracellular and secreted hepatitis C virus particles. *J*  
781 *Viro* **80**:11074-11081.
- 782 38. **Langmead B, Trapnell C, Pop M, Salzberg SL.** 2009. Ultrafast and memory-  
783 efficient alignment of short DNA sequences to the human genome. *Genome*  
784 *Biol* **10**:R25.
- 785 39. **Chen CJ, Servant N, Toedling J, Sarazin A, Marchais A, Duvernois-**  
786 **Berthet E, Cognat V, Colot V, Voinnet O, Heard E, Ciaudo C, Barillot E.**  
787 2012. ncPRO-seq: a tool for annotation and profiling of ncRNAs in sRNA-seq  
788 data. *Bioinformatics* **28**:3147-3149.
- 789 40. **Love MI, Huber W, Anders S.** 2014. Moderated estimation of fold change  
790 and dispersion for RNA-seq data with DESeq2. *Genome Biol* **15**:550.
- 791 41. **Dembele D, Kastner P.** 2014. Fold change rank ordering statistics: a new  
792 method for detecting differentially expressed genes. *BMC Bioinformatics*  
793 **15**:14.

- 794 42. **Liberzon A, Subramanian A, Pinchback R, Thorvaldsdottir H, Tamayo P,**  
795 **Mesirov JP.** 2011. Molecular signatures database (MSigDB) 3.0.  
796 *Bioinformatics* **27**:1739-1740.
- 797 43. **Subramanian A, Tamayo P, Mootha VK, Mukherjee S, Ebert BL, Gillette**  
798 **MA, Paulovich A, Pomeroy SL, Golub TR, Lander ES, Mesirov JP.** 2005.  
799 Gene set enrichment analysis: a knowledge-based approach for interpreting  
800 genome-wide expression profiles. *Proc Natl Acad Sci U S A* **102**:15545-  
801 15550.
- 802 44. **Lu TP, Lee CY, Tsai MH, Chiu YC, Hsiao CK, Lai LC, Chuang EY.** 2012.  
803 miRSystem: an integrated system for characterizing enriched functions and  
804 pathways of microRNA targets. *PLoS One* **7**:e42390.
- 805 45. **Tuddenham L, Jung JS, Chane-Woon-Ming B, Dolken L, Pfeffer S.** 2012.  
806 Small RNA deep sequencing identifies microRNAs and other small noncoding  
807 RNAs from human herpesvirus 6B. *J Virol* **86**:1638-1649.
- 808 46. **Raychaudhuri S, Fontanes V, Barat B, Dasgupta A.** 2009. Activation of  
809 ribosomal RNA transcription by hepatitis C virus involves upstream binding  
810 factor phosphorylation via induction of cyclin D1. *Cancer Res* **69**:2057-2064.
- 811 47. **Chen Y, Chen J, Wang H, Shi J, Wu K, Liu S, Liu Y, Wu J.** 2013. HCV-  
812 induced miR-21 contributes to evasion of host immune system by targeting  
813 MyD88 and IRAK1. *PLoS Pathog* **9**:e1003248.
- 814 48. **Jiang J, Gusev Y, Aderca I, Mettler TA, Nagorney DM, Brackett DJ,**  
815 **Roberts LR, Schmittgen TD.** 2008. Association of MicroRNA expression in  
816 hepatocellular carcinomas with hepatitis infection, cirrhosis, and patient  
817 survival. *Clin Cancer Res* **14**:419-427.

- 818 49. **Marquez RT, Bandyopadhyay S, Wendlandt EB, Keck K, Hoffer BA, Icardi**  
819 **MS, Christensen RN, Schmidt WN, McCaffrey AP.** 2010. Correlation  
820 between microRNA expression levels and clinical parameters associated with  
821 chronic hepatitis C viral infection in humans. *Lab Invest* **90**:1727-1736.
- 822 50. **Meng F, Henson R, Wehbe-Janek H, Ghoshal K, Jacob ST, Patel T.** 2007.  
823 MicroRNA-21 regulates expression of the PTEN tumor suppressor gene in  
824 human hepatocellular cancer. *Gastroenterology* **133**:647-658.
- 825 51. **Bao L, Yan Y, Xu C, Ji W, Shen S, Xu G, Zeng Y, Sun B, Qian H, Chen L,**  
826 **Wu M, Su C, Chen J.** 2013. MicroRNA-21 suppresses PTEN and hSulf-1  
827 expression and promotes hepatocellular carcinoma progression through  
828 AKT/ERK pathways. *Cancer Lett* **337**:226-236.
- 829 52. **Shirasaki T, Honda M, Shimakami T, Horii R, Yamashita T, Sakai Y, Sakai**  
830 **A, Okada H, Watanabe R, Murakami S, Yi M, Lemon SM, Kaneko S.** 2013.  
831 MicroRNA-27a regulates lipid metabolism and inhibits hepatitis C virus  
832 replication in human hepatoma cells. *J Virol* **87**:5270-5286.
- 833 53. **Singaravelu R, Chen R, Lyn RK, Jones DM, O'Hara S, Rouleau Y, Cheng**  
834 **J, Srinivasan P, Nasheri N, Russell RS, Tyrrell DL, Pezacki JP.** 2014.  
835 Hepatitis C virus induced up-regulation of microRNA-27: a novel mechanism  
836 for hepatic steatosis. *Hepatology* **59**:98-108.
- 837 54. **Taganov KD, Boldin MP, Chang KJ, Baltimore D.** 2006. NF-kappaB-  
838 dependent induction of microRNA miR-146, an inhibitor targeted to signaling  
839 proteins of innate immune responses. *Proc Natl Acad Sci U S A* **103**:12481-  
840 12486.

- 841 55. **Bala S, Tilahun Y, Taha O, Alao H, Kodys K, Catalano D, Szabo G.** 2012.  
842 Increased microRNA-155 expression in the serum and peripheral monocytes  
843 in chronic HCV infection. *J Transl Med* **10**:151.
- 844 56. **Zhang Z, Zhang Y, Sun XX, Ma X, Chen ZN.** 2015. microRNA-146a inhibits  
845 cancer metastasis by downregulating VEGF through dual pathways in  
846 hepatocellular carcinoma. *Mol Cancer* **14**:5.
- 847 57. **Qian H, Deng X, Huang ZW, Wei J, Ding CH, Feng RX, Zeng X, Chen YX,**  
848 **Ding J, Qiu L, Hu ZL, Zhang X, Wang HY, Zhang JP, Xie WF.** 2015. An  
849 HNF1alpha-regulated feedback circuit modulates hepatic fibrogenesis via the  
850 crosstalk between hepatocytes and hepatic stellate cells. *Cell Res* **25**:930-  
851 945.
- 852 58. **Cameron JE, Yin Q, Fewell C, Lacey M, McBride J, Wang X, Lin Z,**  
853 **Schaefer BC, Flemington EK.** 2008. Epstein-Barr virus latent membrane  
854 protein 1 induces cellular MicroRNA miR-146a, a modulator of lymphocyte  
855 signaling pathways. *J Virol* **82**:1946-1958.
- 856 59. **Ma X, Becker Buscaglia LE, Barker JR, Li Y.** 2011. MicroRNAs in NF-  
857 kappaB signaling. *J Mol Cell Biol* **3**:159-166.
- 858 60. **Gong G, Waris G, Tanveer R, Siddiqui A.** 2001. Human hepatitis C virus  
859 NS5A protein alters intracellular calcium levels, induces oxidative stress, and  
860 activates STAT-3 and NF-kappa B. *Proc Natl Acad Sci U S A* **98**:9599-9604.
- 861 61. **Sanda T, Iida S, Ogura H, Asamitsu K, Murata T, Bacon KB, Ueda R,**  
862 **Okamoto T.** 2005. Growth inhibition of multiple myeloma cells by a novel  
863 I kappa B kinase inhibitor. *Clin Cancer Res* **11**:1974-1982.
- 864 62. **Zhang HX, Liu ZX, Sun YP, Zhu J, Lu SY, Liu XS, Huang QH, Xie YY, Zhu**  
865 **HB, Dang SY, Chen HF, Zheng GY, Li YX, Kuang Y, Fei J, Chen SJ, Chen**

- 866 **Z, Wang ZG.** 2013. Rig-I regulates NF-kappaB activity through binding to Nf-  
867 kappaB1 3'-UTR mRNA. Proc Natl Acad Sci U S A **110**:6459-6464.
- 868 63. **Li WC, Ye SL, Sun RX, Liu YK, Tang ZY, Kim Y, Karras JG, Zhang H.**  
869 2006. Inhibition of growth and metastasis of human hepatocellular carcinoma  
870 by antisense oligonucleotide targeting signal transducer and activator of  
871 transcription 3. Clin Cancer Res **12**:7140-7148.
- 872 64. **Cantor JR, Sabatini DM.** 2012. Cancer cell metabolism: one hallmark, many  
873 faces. Cancer Discov **2**:881-898.
- 874 65. **Hoshida Y, Fuchs BC, Bardeesy N, Baumert TF, Chung RT.** 2014.  
875 Pathogenesis and prevention of hepatitis C virus-induced hepatocellular  
876 carcinoma. J Hepatol **61**:S79-90.
- 877 66. **Zhu K, Pan Q, Zhang X, Kong LQ, Fan J, Dai Z, Wang L, Yang XR, Hu J,**  
878 **Wan JL, Zhao YM, Tao ZH, Chai ZT, Zeng HY, Tang ZY, Sun HC, Zhou J.**  
879 2013. MiR-146a enhances angiogenic activity of endothelial cells in  
880 hepatocellular carcinoma by promoting PDGFRA expression. Carcinogenesis  
881 **34**:2071-2079.
- 882 67. **Sun X, Zhang J, Hou Z, Han Q, Zhang C, Tian Z.** 2015. miR-146a is directly  
883 regulated by STAT3 in human hepatocellular carcinoma cells and involved in  
884 anti-tumor immune suppression. Cell Cycle **14**:243-252.
- 885 68. **Peng Q, Li S, Lao X, Chen Z, Li R, Deng Y, Qin X.** 2014. The association of  
886 common functional polymorphisms in mir-146a and mir-196a2 and  
887 hepatocellular carcinoma risk: evidence from a meta-analysis. Medicine  
888 (Baltimore) **93**:e252.
- 889 69. **Li JF, Dai XP, Zhang W, Sun SH, Zeng Y, Zhao GY, Kou ZH, Guo Y, Yu H,**  
890 **Du LY, Jiang SB, Zhou YS.** 2015. Upregulation of microRNA-146a by

- 891 hepatitis B virus X protein contributes to hepatitis development by  
892 downregulating complement factor H. *MBio* **6**: doi: 10.1128/mBio.02459-14.
- 893 70. **Huang S, He R, Rong M, Dang Y, Chen G.** 2014. Synergistic effect of MiR-  
894 146a mimic and cetuximab on hepatocellular carcinoma cells. *Biomed Res Int*  
895 **2014**:384121.
- 896 71. **Suzuki R, Matsuda M, Watashi K, Aizaki H, Matsuura Y, Wakita T, Suzuki**  
897 **T.** 2013. Signal peptidase complex subunit 1 participates in the assembly of  
898 hepatitis C virus through an interaction with E2 and NS2. *PLoS Pathog*  
899 **9**:e1003589.
- 900 72. **Yamaguchi A, Tazuma S, Nishioka T, Ohishi W, Hyogo H, Nomura S,**  
901 **Chayama K.** 2005. Hepatitis C virus core protein modulates fatty acid  
902 metabolism and thereby causes lipid accumulation in the liver. *Dig Dis Sci*  
903 **50**:1361-1371.
- 904 73. **Syed GH, Amako Y, Siddiqui A.** 2010. Hepatitis C virus hijacks host lipid  
905 metabolism. *Trends Endocrinol Metab* **21**:33-40.
- 906 74. **Ramiere C, Rodriguez J, Enache LS, Lotteau V, Andre P, Diaz O.** 2014.  
907 Activity of hexokinase is increased by its interaction with hepatitis C virus  
908 protein NS5A. *J Virol* **88**:3246-3254.

909  
910  
911

912 **Figure legends**

913 **Figure 1. Persistent HCV infection modulates host cell miRNA expression in**

914 **hepatocyte-like Huh7.5.1 cells.** (A-B) Huh7.5.1 cells were differentiated into

915 hepatocyte-like cells using 1% DMSO (14-16), persistently infected using HCVcc and

916 subject to molecular analyses at 7 days post-infection (dpi). (A) Immuno-detection of

917 HCV E2 protein in HCV Jc1-infected hepatocyte-like cells (HCV) and non-infected

918 controls (Control). Nuclei are counterstained with DAPI. Representative overlay

919 images are shown. Scale bar, 50  $\mu$ m. (B) Modulation of miRNA expression by HCV

920 infection. Small RNAs (19-24 nt) from HCV Jc1E2<sup>FLAG</sup>-infected cells (HCV) or non-

921 infected controls (Control) were subject to RNA-Seq (Material and Methods). The

922 scatter plot shows the 72 miRNAs with significant modulation upon HCV infection as

923 compared to control cells (red dots). miR-21-5p, miR-146a-5p and miR-143-3p

924 presenting enrichment in HCV-infected cells are highlighted in blue. (C) HCV

925 increases the expression of miR-21-5p, miR-146a-5p and miR-143-3p in hepatocyte-

926 like cells. miRNA expression was analyzed by RT-qPCR in total RNA extracts from

927 HCV-infected cells as compared to non-infected controls. Results are from three

928 independent experiments. (D) HCV increases the expression of miR-21-5p, miR-

929 146a-5p and miR-143-3p in PHH. miRNA expression was analyzed by RT-qPCR in

930 total RNA extracts from HCV Jc1-infected PHH at 3 dpi as compared to non-infected

931 controls. Results are from five independent experiments. In C and D, the plots show

932 the sample lower quartile (25th percentile; bottom of the box), the median (50th

933 percentile; horizontal line in box) and the upper quartile (75th percentile; top of the

934 box). The whiskers indicate the 2.5 and 97.5 percentile, respectively. (E) miR-146a-

935 5p expression is enhanced in liver tissue from HCV-infected patients. Liver tissues

936 from 20 HCV-infected patients (HCV) and 9 non-infected subjects (Control) were

937 analyzed for miR-146a-5p expression by RT-qPCR. Results from each biopsy are  
938 shown as dots. Median miRNA expression is shown as black lines. (F) The HCV-  
939 induced up-regulation of miR-146a-5p is mediated by NF- $\kappa$ B in hepatocyte-like cells.  
940 Cells were pre-treated using IKK inhibitor ACHP (6.25  $\mu$ M) for 24 h and subjected or  
941 not to HCV infection for 5 days. Non-treated cells (Control) were analyzed in parallel.  
942 miR-146a-5p expression was assessed by RT-qPCR. The plots show mean fold  
943 change  $\pm$  s.e.m. from 4 independent experiments. In C, D and E \* $p$ <0.05, \*\* $p$ <0.01  
944 and \*\*\* $p$ <0.0001 two-tailed Mann-Whitney test; in F, \* $p$ <0.01 and \*\* $p$ <0.001 one-way  
945 ANOVA.

946

947 **Figure 2. Over-expression of miR-146a-5p does not alter proliferation and cell**  
948 **cycle distribution in hepatocyte-like cells.** Differentiated Huh7.5.1 cells were  
949 transfected using control siRNA, miR-146a-5p mimic or siSTAT3. (A) Cell  
950 proliferation was assessed 24, 48, 72 and 96 hours after transfection by direct cell  
951 counting. The plots show the sample lower quartile (25th percentile; bottom of the  
952 box), the median (50th percentile; horizontal line in box) and the upper quartile (75th  
953 percentile; top of the box). The whiskers indicate the 2.5 and 97.5 percentile,  
954 respectively. Results are from three independent experiments, \* $p$ <0.05, \*\* $p$ <0.01  
955 Kruskal-Wallis H test; ns, not significant. (B) Cell cycle distribution was assessed at  
956 the different time points using flow cytometry following propidium iodide staining.  
957 Representative cell cycle profiles from one out of three independent experiments are  
958 shown. '2C' indicates cells in G0/G1 phase having diploid DNA content while '4C'  
959 indicates cells in G2/M phase having tetraploid DNA content. The population of miR-  
960 146a-5p over-expressing cells displays a comparable profile to that of control cells. In

961 contrast, the number of cells in S and G2/M phase is markedly decreased upon  
962 knock-down of *STAT3* as compared with controls.

963

964 **Figure 3. miR-146a-5p modulates the expression of genes related to liver**  
965 **disease.** (A) Modulation of mRNA expression by miR-146a-5p in hepatocyte-like  
966 cells. Hepatocyte-like cells were reverse transfected with miR-146a-5p mimic or non-  
967 targeting control (5 nM) three days prior to total RNA extraction and analysis of  
968 mRNA expression by microarray. Gene expression profiles are represented as a  
969 volcano plot where the x-axis represents the log<sub>2</sub> of the fold change between miR-  
970 146a-5p-transfected cells and control cells, and the y-axis represents the -log<sub>10</sub> of  
971 the p-value obtained from the f-cross test comparing miR-146a-5p-transfected cells  
972 to control cells. Red dots represent mRNA considered statistically significant  
973 ( $p < 0.015$ , FCROS method). (B) Functional network analysis of the genes with  
974 modified expression after miR-146a-5p over-expression in hepatocyte-like cells. IPA-  
975 toxicity algorithm was used to assess the enrichment of the deregulated genes in  
976 specific toxicity pathways with altered expression in human disease. The  $p$ -value  
977 indicates the significance of the enrichment of the input genes for each *Tox function*  
978 pathway. (C) Co-regulated gene networks in miR-146a-5p over-expressing cells.  
979 Modulation of molecular pathways by miR-146a-5p was determined in KEGG  
980 database using GSEA (43). Significantly enriched gene networks involved in immune  
981 responses (in blue), cell cycle and DNA repair (in black) as well as cell metabolism  
982 (in grey) are shown. Gene sets down-regulated by miR-146a-5p are depicted as  
983 open circles while gene sets up-regulated by the miRNA are represented as black  
984 circles. The thickness of the connecting lines is proportional to the degree of  
985 overlapping genes between two different gene sets.

986 **Figure 4. Eradication of HCV infection does not restore the HCV-mediated over-**  
987 **expression of miR-146a-5p.** Persistently HCV (Jc1E2<sup>FLAG</sup>)-infected hepatocyte-like  
988 cells were treated or not using a combination of DAAs (5 nM DCV, 1  $\mu$ M SOF and 0.5  
989  $\mu$ M SMV). Non-infected cells were analyzed as controls. (A) After 4 weeks of DAA-  
990 treatment followed by 2 weeks of washout, HCV RNA load was assessed by RT-  
991 qPCR in cell supernatants from HCV-infected non-treated cells (HCV) or HCV-  
992 infected DAA-treated cells (HCV + DAAs). The limit of quantification (LOQ), indicated  
993 by a dashed line, was  $10^3$  copies/mL. Results from 4 biological replicates are shown.  
994 Median HCV loads are shown as black lines. The cross indicates one sample that  
995 was HCV RNA negative. (B) miR-146a-5p expression was analyzed by RT-qPCR in  
996 total RNA extracts from the same samples as well as non-infected control cells. The  
997 plots show the sample lower quartile (25th percentile; bottom of the box), the median  
998 (50th percentile; horizontal line in box) and the upper quartile (75th percentile; top of  
999 the box). The whiskers indicate the 2.5 and 97.5 percentile, respectively. The red  
1000 dashed line indicates a fold-change = 1. In A and B, \* $p < 0.05$ , two-tailed Mann-  
1001 Whitney test; nd, not determined; ns, not significant.

1002

1003 **Figure 5. miR-146a-5p promotes HCV infection by enhancing production of**  
1004 **infectious viral particles.** (A) miR-146a-5p does not affect HCV entry. Huh7.5.1  
1005 cells were transfected with the indicated compounds and incubated with HCVpp for  
1006 72h. HCVpp entry was assessed by determining intracellular luciferase activity  
1007 expressed as relative light units (RLU). Results represent mean percentage  $\pm$  s.d.  
1008 from three independent experiments. (B) miR-146a-5p decreases HCV RNA  
1009 translation. Huh7.5.1 cells were transfected with the indicated compounds and 48h  
1010 later transfected with HCV RNA (JcR2a). HCV translation was assessed by

1011 determination of luciferase activity 4h later. Results are shown as mean percentage  $\pm$   
1012 s.d. from three independent experiments. (C) miR-146a-5p does not modulate HCV  
1013 replication. Huh7.5.1 cells were electroporated with assembly-deficient JFH1/ $\Delta$ E1E2  
1014 RNA 48h prior to transfection with the indicated compounds. HCV replication was  
1015 assessed by determination of luciferase activity 48h later. Results are shown as  
1016 mean percentage  $\pm$  s.d. from four independent experiments. In A, B and C the  
1017 dashed line indicates RLU = 100 % of control. (D-E) miR-146a promotes HCV  
1018 assembly and egress. Huh7.5.1 were transfected with the indicated compounds 48h  
1019 prior to infection with HCVcc (Jc1). After 4h, the viral inoculum was removed and  
1020 cells were incubated with fresh medium for 48h. Cells were lysed to determine  
1021 intracellular HCV RNA load and infectivity (TCID<sub>50</sub>/mL). Likewise, supernatants were  
1022 used to determine the extracellular HCV RNA load and infectivity. Results represent  
1023 (D) extracellular and (E) intracellular HCV infectivity as fold change compared to  
1024 control-transfected cells and are from nine independent experiments. The plots show  
1025 the sample lower quartile (25th percentile; bottom of the box), the median (50th  
1026 percentile; horizontal line in box) and the upper quartile (75th percentile; top of the  
1027 box). The whiskers indicate the 2.5 and 97.5 percentile, respectively. The dashed line  
1028 indicates a fold-change = 1. In A, B and C, \* $p$ <0.001 and \*\* $p$ <0.0001 unpaired t-test  
1029 with Welch's correction; in D and E \* $p$ <0.05, \*\* $p$ <0.01 and \*\*\* $p$ <0.0001 two-tailed  
1030 Mann-Whitney test.

1031 **Table 1. Characteristics of the patients and patient-derived liver biopsies**  
 1032 **included in the study**

Biopsy ID	HCV genotype	Viral Load (x 10 <sup>6</sup> IU/mL)	Diagnosis	Metavir	Age at biopsy (years)	Gender
C270	1b	1.8	Chronic HCV infection	A3/F3	76	F
C238	1b	nd	Chronic HCV infection	A1/F1	54	F
C257	1a	0.1	Chronic HCV infection	A1/F1	30	M
B823	4	3.2	Chronic HCV infection	A1/F1	50	M
C669	3a	19.9	Chronic HCV infection	A2/F2	48	M
C672	4	11.9	Chronic HCV infection	A1/F1	45	M
C561	1b	1.1	Chronic HCV infection	A3/F3	70	M
C579	1a	1.10	Chronic HCV infection	A2/F3	50	M
C703	1b	nd	Chronic HCV infection	A2/F2	48	F
C716	3a	3.5	Chronic HCV infection	A3/F4	49	F
C582	1a	2.9	Chronic HCV infection	A2/F2	60	F
C748	1a	9.4	Chronic HCV infection	A1/F2	56	M
C567	1b	1.3	Chronic HCV infection	A2/F3	64	F
C757	1	2	Chronic HCV infection	A1/F2	71	F
C685	3a	4.7	Chronic HCV infection	A1/F2	55	F
C651	4	1.2	Chronic HCV infection	A1/F1	55	M
C663	4	nd	Chronic HCV infection	A2/F3	55	M
C766	1a	0.4	Chronic HCV infection	A1/F1	40	F
C262	n/a	n/a	ASH, cirrhosis	n/a	59	F
C344	n/a	n/a	Steatosis 5%, siderosis grade I	n/a	43	M
C332	n/a	n/a	NASH	n/a	49	F
C330	n/a	n/a	Minimal steatosis	n/a	47	M
C305	n/a	n/a	Minimal unspecific hepatitis	n/a	44	M
C298	n/a	n/a	Steatohepatitis (NASH)	n/a	50	M
C237	n/a	n/a	Steatosis, ASH, siderosis	n/a	51	M
C187	n/a	n/a	Normal liver parenchymal	n/a	31	F
C145	n/a	n/a	Normal liver parenchymal	n/a	43	F

1033

1034 ASH, alcoholic steatohepatitis; F, Female; M, Male; HCV, HCV-infected patient; n/a,

1035 non applicable; NASH, nonalcoholic steatohepatitis; nd, not determined.

1036  
1037

**Table 2. HCV-regulated miRNAs with a known involvement in inflammation, fibrosis and cancer<sup>a</sup>.**

miRNA ID	miRNA Target (gene symbol)	Molecular function		
		Inflammation	Fibrosis	Cancer
miR-122-5p	IGF1R	x	x	x
	SRF	x	x	x
	CCNG1			x
	SLC7A1			x
	BCL2L2	x		
	ADAM10	x	x	x
	PRKRA			
	WNT1	x	x	x
miR-210-3p	FGFRL1			x
	RAD52		x	x
	EFNA3			x
	BDNF	x	x	x
	PTPN1	x		
	ISCU			x
	E2F3			x
	MNT	x	x	x
miR-338-5p	LRP1	x		x
miR-483-3p	SMAD4	x	x	x
	BBC3			x
	SRF	x	x	x
	MAPK3			x
miR-574-5p	FOXN3			x
miR-885-5p	CDK2		x	x
	MCM5			x
miR-1	HCN4	x		
	FOXP1			x
	HCN2	x	x	
	PTMA			x
	MET	x	x	x
	XPO6			x
	TAGLN2	x	x	x
	LASP1	x		x
	KCNE1			x
	PNP			x
	PIM1	x		x
	PAX3			x
	TWF1		x	x
	TWF2			
	FN1	x		x
	NOTCH3	x	x	
FABP3		x	x	
miR-10a-5p	HOXA1	x		x
	USF2		x	x
	MAP3K7	x		x
	BTRC			

	EPHA4		X		X
miR-127-3p	PRDM1		X		X
	BCL6		X		X
miR-132-3p	CDKN1A		X	X	X
	ARHGAP32				
	RB1		X		X
	HBEGF		X	X	X
miR-133b	KCNH2				X
	FSCN1				X
	FAIM				X
	EGFR		X	X	X
	FGFR1		X	X	X
	HCN4		X		
miR-143-3p	KRAS		X	X	X
	MYO6				X
	DNMT3A		X	X	X
	FNDC3B				X
	MAPK7				X
	FSCN1				X
	SERPINE1		X	X	X
	MACC1		X		X
	JAG1		X	X	X
	AKT1		X	X	X
miR-146a-5p	CXCR4		X	X	X
	TLR2		X	X	X
	TRAF6		X		X
	IRAK1		X		X
	BRCA1		X		X
	NFKB1		X		X
	EGFR		X	X	X
	CD40LG		X	X	X
	SMAD4		X	X	X
	HNF1		X	X	X
	SHP1		X	X	X
	TLR4		X	X	X
miR-150-5p	MYB		X	X	X
	EGR2		X		X
	MUC4		X	X	X
	ZEB1		X	X	X
miR-206	MET		X	X	X
	NOTCH3		X	X	
	ESR1		X		X
	PAX3				X
miR-212-3p	MECP2		X	X	X
	PEA15				X
	PTCH1			X	X
	RB1		X		X
miR-21-5p	RASGRP1				X

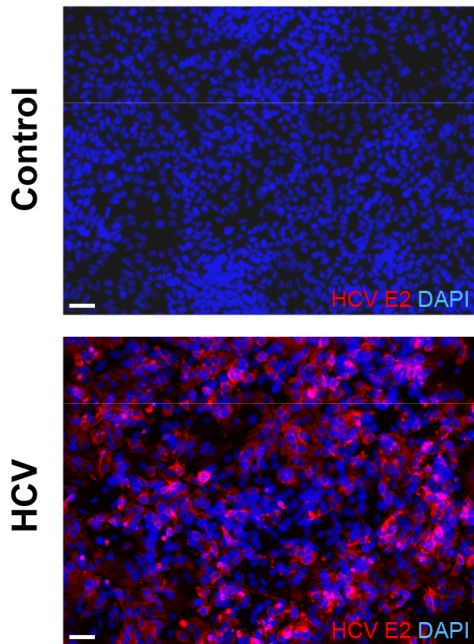
	BCL2	x	x	x
	TIMP3	x	x	x
	SOX5			x
	MTAP	x	x	x
	RECK		x	x
	TGFBR2	x	x	x
	PTEN	x	x	x
	E2F1	x	x	x
	LRRFIP1	x		x
	TPM1			x
	NFIB			x
	APAF1	x		x
	BTG2			x
	PDCD4	x	x	x
	RHOB	x		x
	SERPINB5		x	x
	BMPR2	x	x	x
	DAXX	x		x
	TP63			x
	MSH2	x		x
	MSH6			x
	ISCU			x
	EIF4A2			x
	ANKRD46			x
	CDK2AP1			x
	DUSP10			x
	PPARA	x	x	x
	ANP32A			x
	SMARCA4			x
	FASLG	x	x	x
miR-494-3p	PTEN	x	x	x
	CDK6	x		x
	BCL2L11			x
miR-584-5p	ROCK1	x	x	x
miR-663a	JUNB	x		x
	JUND		x	x

1038

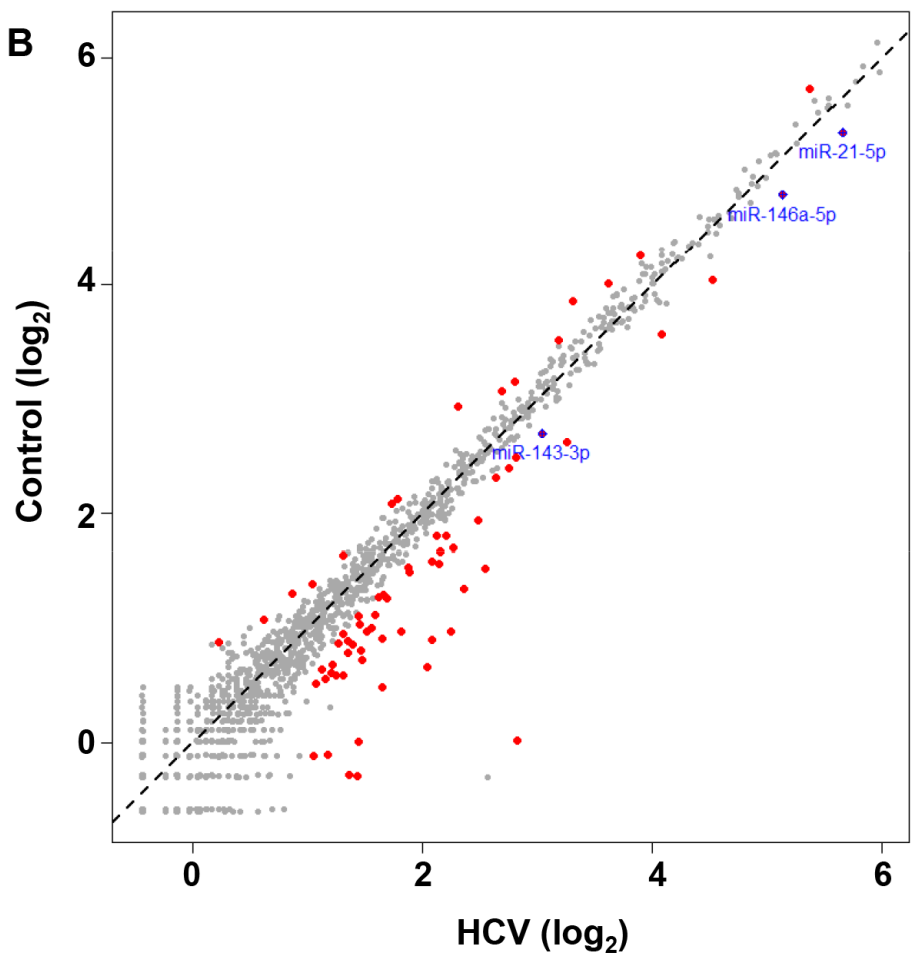
1039 <sup>a</sup>The targets of miRNAs differentially regulated by HCV infection in hepatocyte-like  
1040 Huh7.5.1 cells at 7 days post-infection were retrieved using the miRsystem tool. The  
1041 involvement of these target genes into pathways related to inflammation, fibrosis and  
1042 cancer was assessed through miRsystem and a systematic screen of the available  
1043 literature using PubMed. x: involvement of miRNA target into the indicated process.

Figure 1

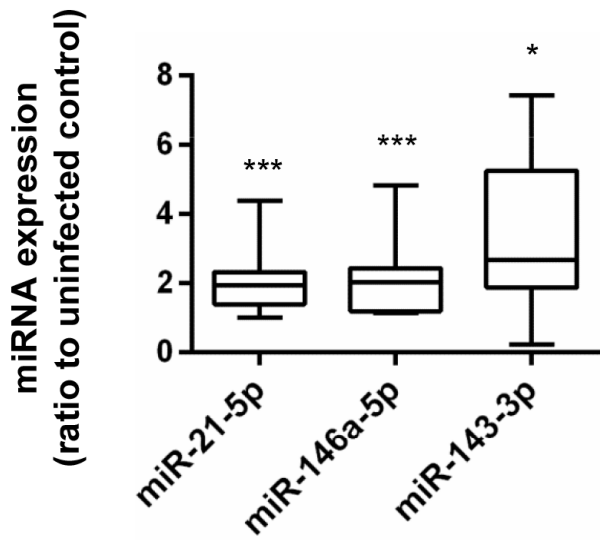
A



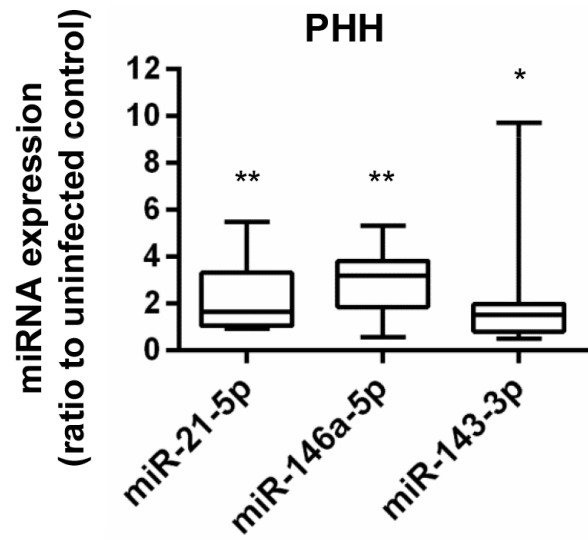
B



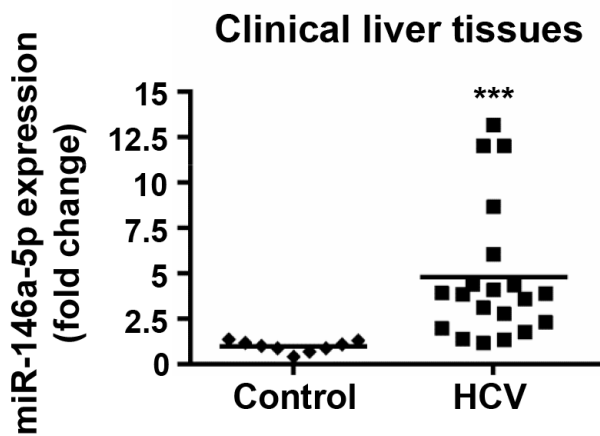
C



D



E



F

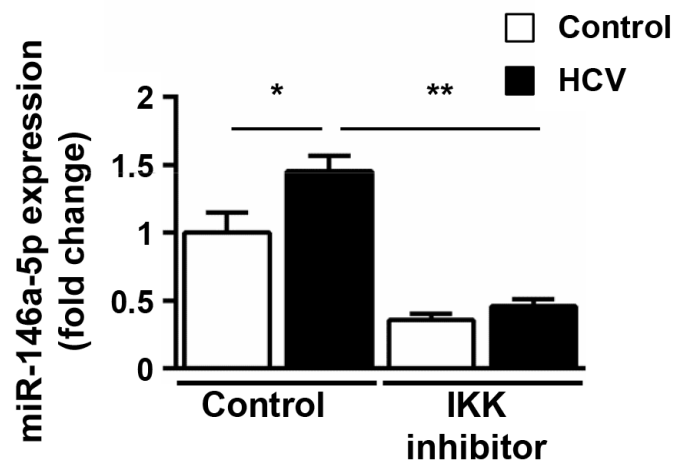
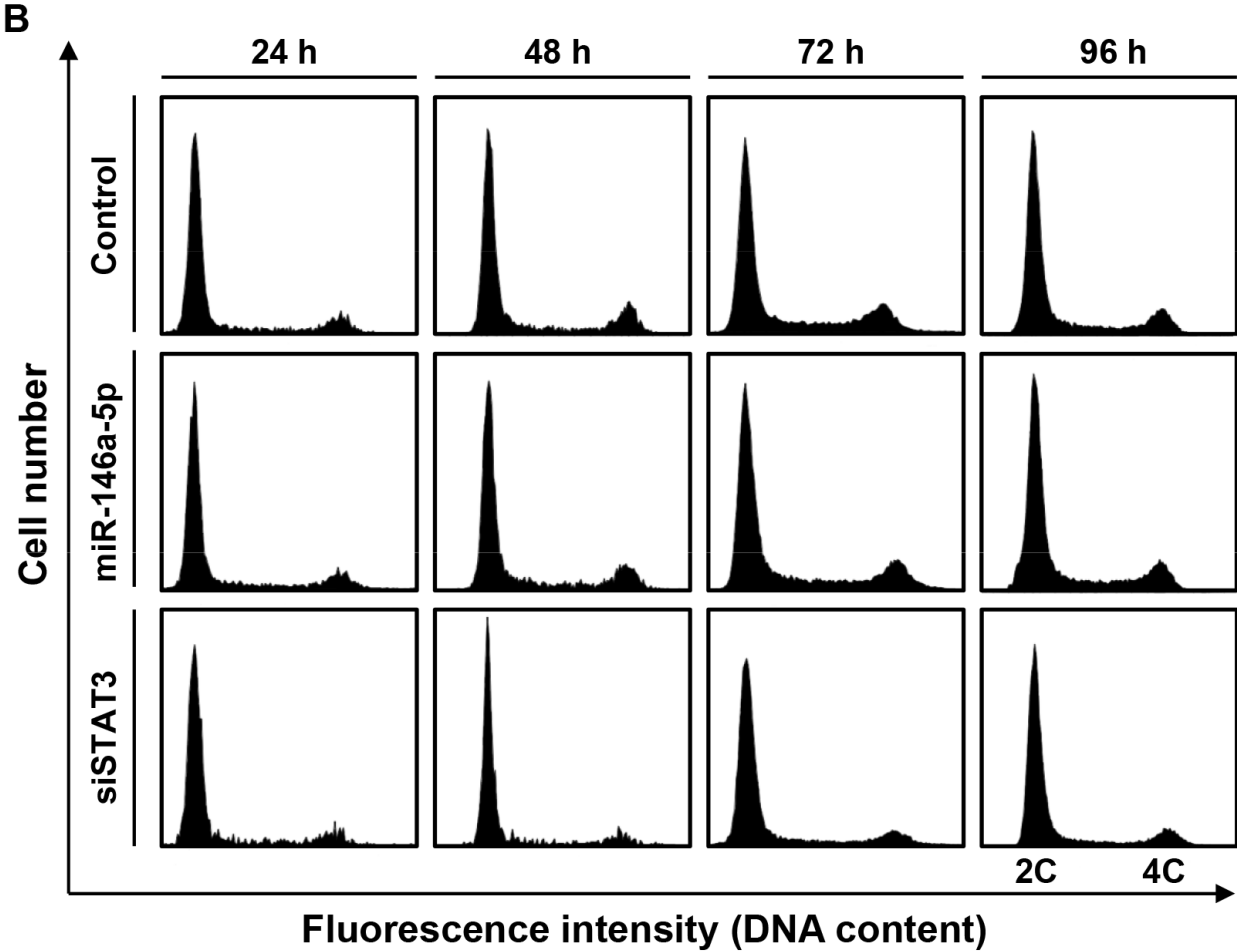
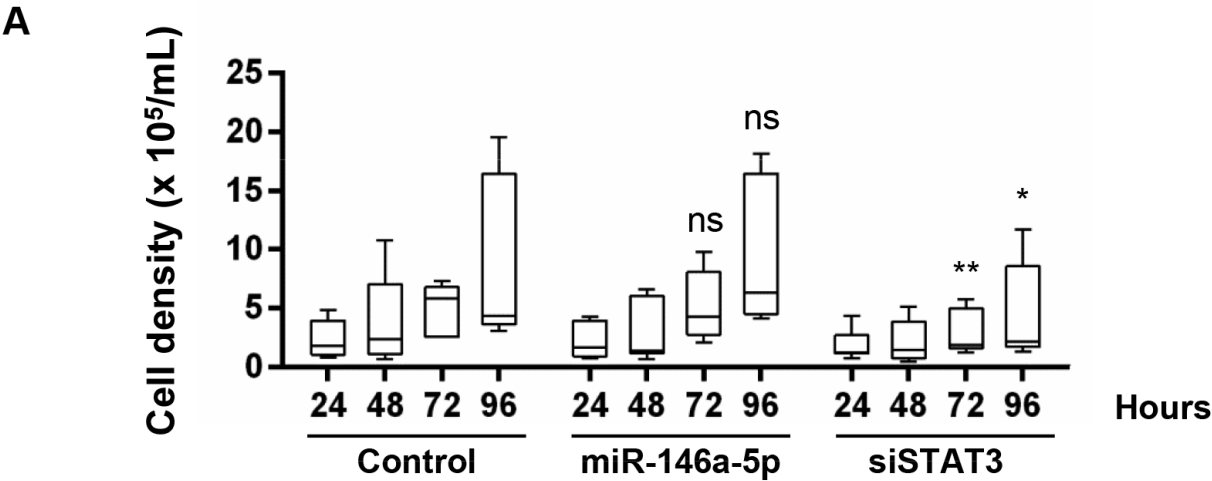


Figure 2



**Figure 3**

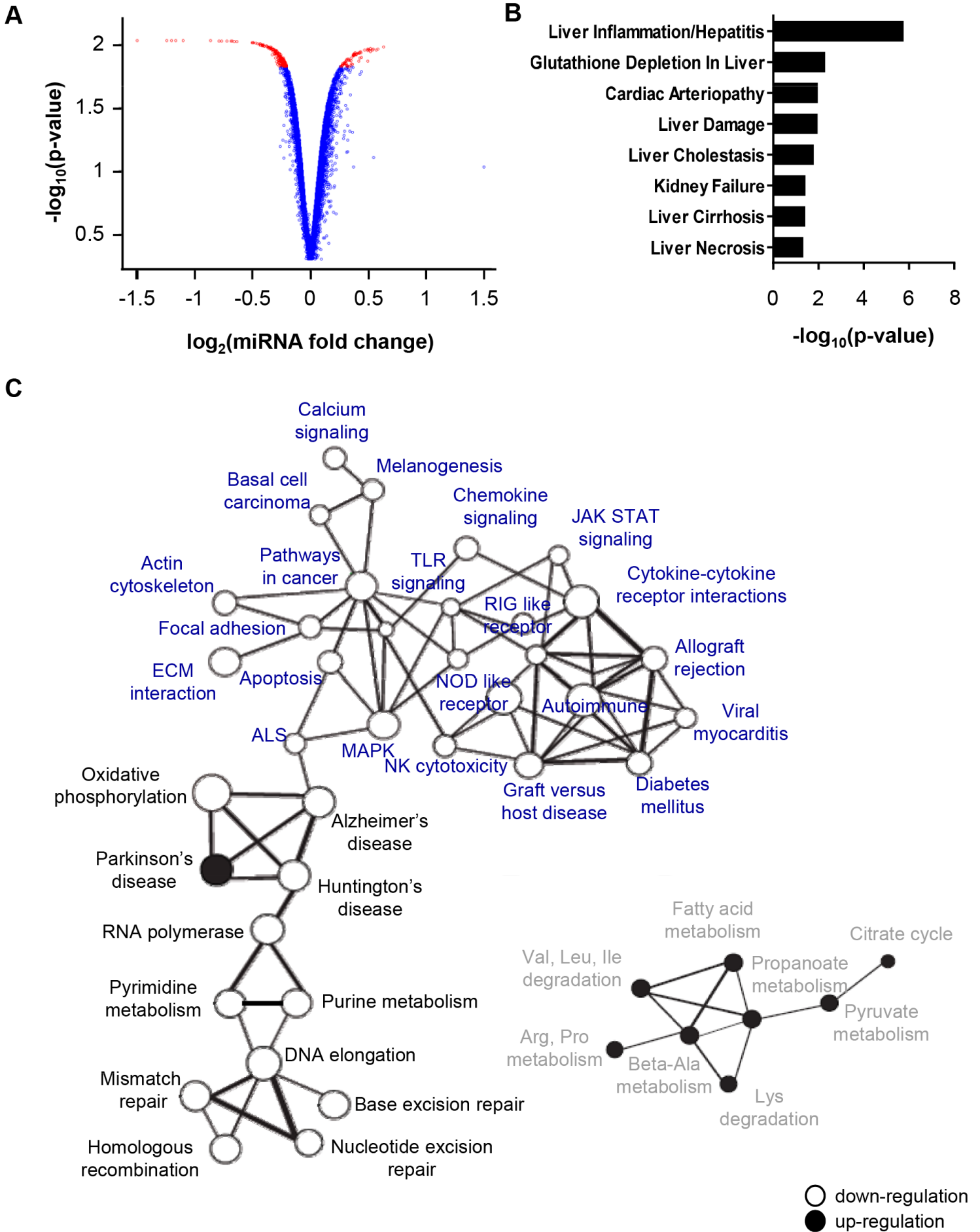
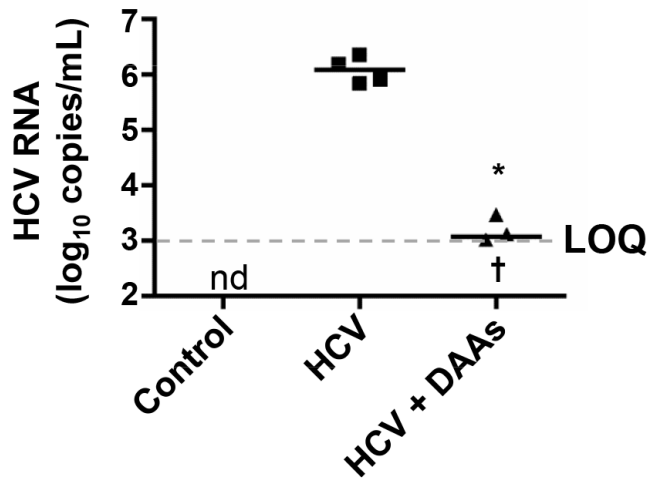


Figure 4

A



B

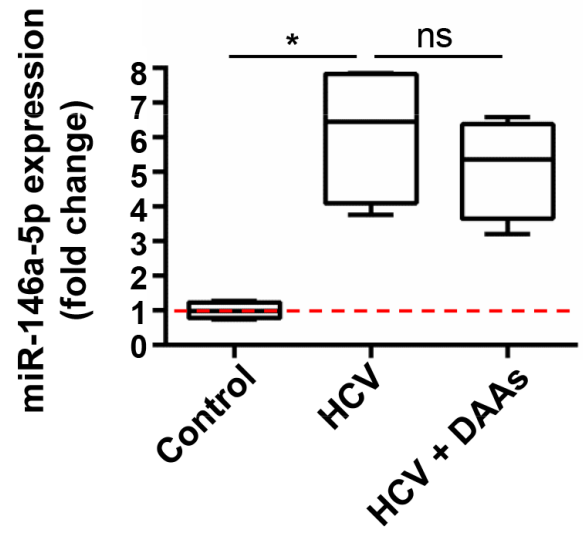


Figure 5

